Tracer testing in the Svartsengi geothermal field in 2015

Sigrún Brá Sverrisdóttir

Thesis of 60 ECTS credits
Master of Science (M.Sc.) in Sustainable Energy Engineering

January 2016

Tracer testing in the Svartsengi geothermal field in 2015

Thesis of 60 ECTS credits submitted to the School of Science and Engineering
at Reykjavík University in partial fulfillment of
the requirements for the degree of
Master of Science (M.Sc.) in Sustainable Energy Engineering

January 2016

Supervisors:

Ágúst Valfells, Supervisor
Associate Professor, Reykjavík University, Iceland

Guðni Axelsson, Co-advisor
Reservoir Engineer, ÍSOR, Iceland

Examiner:

Egill Júlíusson, Examiner
Reservoir Engineer, Landsvirkjun, Iceland

Tracer testing in the Svartsengi geothermal field in 2015

Sigrún Brá Sverrisdóttir

January 2016

Abstract

The Svartsengi geothermal field has been utilized for district heating since 1976 and electricity generation since 1980. Some complications due to the utilization have arisen throughout the years. Those include a rapid pressure drawdown in the field and issues regarding waste water management. The continuous injection of spent geothermal fluid began in 1998 when SV-17 was taken into use. With the addition of SV-24 as an injection well in 2008, the injection rate was slowly increased to 60% of the extraction rate. Pressure measurements showed that the injection provided pressure support to the field, but the addition of a new energy plant and increased production from the field reintroduced the trend of declining field pressure. An important part of geothermal field management is to monitor injection wells and study the ability to increase reinjection. In the summer of 2015 a threefold tracer test was performed in Svartsengi for that purpose. Liquid phase tracers were injected into wells SV-17 and SV-24, 2,7-napthalene disulfonate and 2,6-napthalene disuldonate, and a steam tracer, sulfurhexafluoride, was injected into SV-24. Samples have since been taken from all production wells in the field with the addition of the monitoring well in Eldvörp. At the time of writing the 2,6-NDS has only been detected in well SV-9, while no signs have been noted of 2,7-NDS. However, the steam tracer has been detected in all production wells and sampling for that has been terminated, but no signs were detected in the well in Eldvörp. The tracer returns were modelled quantitatively using a couple of programs from the ICEBOX software package from ÍSOR. TRINV was used to simulate the tracer recovery based on the theory of solute transport and one dimensional flow channel models. TRCOOL was used to predict the cooling in the production wells due to the injection. Only 0.035% of the injected steam phase tracer was recovered in the production wells, indicating a very modest recharge from the injection well to the production wells. Well SV-23 had the largest tracer recovery, but SV-11 experienced the highest tracer concentration. Cooling predictions were calculated for the current injection scenario in well SV-24 and for a scenario where the current injection rate was doubled, for 30 years. For both scenarios the model predicted an insignificant cooling in production wells over the 30 year period.

Úrvinnsla á ferilefnaprófunum í Svartsengi 2015

Sigrún Brá Sverrisdóttir

janúar 2016

Útdráttur

Vinnsla úr jarðhitasvæðinu Svartsengi hófst árið 1976 þegar heitu vatni var hleypt á fyrstu húsin í Grindavík. Fjórum árum síðar hófst raforkuframleiðsla úr svæðinu, þegar orkuver III var tekið í notkun. Með stöðugri framleiðslu hafa nokkur stærri vandmál litið dagsins ljós. Þar á meðal má nefna; hröð þrýstingslækkun vegna vinnslu og losun jarðsjávar á yfirborð. Til að stemma stigu við þessum vandamálum hófst stöðug niðurdæling í holu SV-17 árið 1998. Tíu árum seinna var annarri niðurdælingarholu bætt við, SV-24, og í hægum skrefum var niðurdæling aukin í 60% af upptöku úr svæðinu. Þrýstingsmælingar sýndu að niðurdælingin dró verulega úr hraða þrýstingslækkunarinnar í vinnsluholum, en þegar orkuver VI tók til starfa jókst þrýstingslækkun í Svartsengi á ný. Hluti af rekstri jarðhitasvæða er að rannsaka áhrif niðurdælingar á svæðið og kanna möguleika á aukinni niðurdælingu. Í þeim tilgangi hófst þríþátta ferilefnapróf sumarið 2015. Vökvafasa ferilefni voru sett niður í holur SV-17 og SV-24, 2,7-napthalene disulfonate og 2,6-napthalene disulfonate. Gufufasa ferilefnið sulfuhexafluoríð var sett niður í holu SV-24. Sýni voru síðan tekin úr öllum vinnslu holum í Svartsengi ásamt rannsóknar holu í Eldvörp. Þegar þetta er skrifað, hefur vökvafasa ferilefnið sem sett var niður í holu SV-24 einungis greinst í tveimur sýnum frá einni holu, SV-9, en gufufasa efnið hefur lokið komu sinni í allar vinnsluholur. Enn hefur ekki greinst 2,7-napthalene disulfonat. Engin merki um sulfurhexafluoríð voru merkjanleg í Eldvörp. Endurheimtur gufufasans voru hermdar í forritum sem fáanleg eru í ICEBOX forritapakkanum frá ÍSOR. TRINV var notað til að herma rennslisleiðir milli niðurdælingar holunnar og vinnsluholanna. TRCOOL var hinsvegar notað til að reikna út áætlaða kólnun svæðisins vegna niðurdælingar. Einungis 0,035% af ferlefninu sem var dælt niður var endurheimt í vinnsluholunum. Það benti til þess að einungis örlítill hluti af niðurdældavökvanum skilaði sér í þær holur sem vinna úr gufuhluta svæðisins. Stærsti hluti ferilefnisins var endurheimtur í holu SV-23, en hæsti styrkur efnisins kom fram í holu SV-11. Gerðar voru kólnunarspár fyrir núverandi niðurdælingu í 30 ár, ásamt tvöföldu magni þess sem nú er dælt niður. Báðar spár bentu til þess að niðurdæling í 30 ár myndi ekki hafa marktæk áhrif á núverandi hitastig svæðisins.

Tracer testing in the Svartsengi geothermal field in 2015

Sigrún Brá Sverrisdóttir

Thesis of 60 ECTS credits submitted to the School of Science and Engineering
at Reykjavík University in partial fulfillment of
the requirements for the degree of
Master of Science (M.Sc.) in Sustainable Energy Engineering

January 2016

Student:

.....

Sigrún Brá Sverrisdóttir

Supervisors:

.....

Ágúst Valfells

.....

Guðni Axelsson

Examiner:

.....

Egill Júlíusson

Acknowledgements

I would like to acknowledge Ágúst Valfells and Guðni Axelsson for their support and guidance throughout this whole process, and my employer HS Orka for trusting me with this project and providing me with all the resources needed to finish the thesis, both financial and informations, Kristín Vala Matthíasdóttir for bringing me the idea this project and all the encouragement throughout the process, Ómar Sigurðsson for working on production numbers and providing valuable feedback, and Kjartan Marteinsson for assisting me with TRINV.

Finally, I want to thank my family for all the support when I needed it the most and special thanks to my boyfriend Rich for his endless support and proofreading.

Contents

List of Figures

List of Tables

List of Abbreviations

HPLC	High performance liquid chromatograph
ÍSOR	Iceland GeoSurvey
NDS	Napthalenedisulfonate
ppb	Parts per billion
ppm	Parts per million

List of Symbols

Symbol	Description
A	Cross-sectional area of flow channel [m^2]
b	Half of the fracture width [meters]
C	Tracer concentration [kg/m^3]
c_f	Specific heat of fracture zone material [J/kg/°C]
c_m	Specific heat of rock matrix [J/kg/°C]
c_R	Specific heat capacity of the rock [J/kg/°C]
c_w	Specific heat of the geothermal fluid [J/kg/°C]
$c(t)$	Tracer concentration in produced fluid [kg/m^3]
$C(t)$	Tracer concentration in flow channel [kg/m^3]
$c(s)$	Tracer concentration in well [kg/L]
D^*	Coefficient of molecular diffusion [m^2/s]
D	Dispersion coefficient [m^2/s]
F_x	Tracer mass flow rate, x-direction [kg/m^2s]
$F_{x,advection}$	Tracer mass flow rate due to advection [kg/m^2s]
$F_{x,dispersion}$	Tracer mass flow rate due to dispersion [kg/m^2s]
h	Height of fracture [m]
h_f	Enthalpy of saturated liquid [kJ/kg]
h_g	Enthalpy of saturated vapor [kJ/kg]
h_geof	Enthalpy of the geothermal fluid [kJ/kg]
k_{th}	Thermal conductivity of the formation [W/m/°C]
L	Flow channel length [m]
m_{empty}	Mass of an empty flask [g]
$m_{evacuated}$	Mass of flask after evacuation [g]
m_{full}	Mass of a full flask [g]
m_{SF_6}	Mass of SF_6
$m_i(t)$	Cumulative tracer return [kg]
M	Injected tracer mass [kg]
$M(SF_6)$	Molar mass of SF_6 [g/mol]
n_{line}	Number of moles in injection line [mol]
n_{SF_6}	Number of SF_6 moles in sample [mol]
n_{total}	Total number of moles in sample [mol]
P_{line}	Pressure in injection line [mbar]
q	Flow in channel [kg/s]
q_{inj}	Injection rate [kg/s]
Q	Production rate [kg/s]
R	Gas constant [83144.7 ml mbar /mol/K]
$R_{thermal}$	Thermal retardation coefficient [-]
t	Time [seconds]

T_f	Temperature of fluid [°C]
T_I	Initial formation temperature [°C]
T_m	Temperature of fluid in fracture [°C]
$T_p(L,t)$	Production temperature[°C]
T_0	Initial formation temperature [°C]
T	Temperature in sampling line [K]
u	Average linear velocity [m/s]
V_f	Volume of sampling flask [ml]
V_{hs}	Volume of flask headspace [ml]
V_{line}	Volume of intake line [l]
V_{total}	Total volume in gas chromatograph [l]
x	Distance along a flow channel [m]
x_v	Vapor quality [-]
α_L	Longitudinal dispersivity of channel [m]
α_x	Dispersivity [m]
ϕ	Porosity [-]
ρ	Density of material [kg/m^3]
π	Pi
κ	Thermal diffusivity [m^2/s]
ω_{inj}	Fraction of injected fluid reaching the production well [-]

Chapter 1

Introduction

The first wells were drilled in the Svartsengi geothermal field in 1971 and continuous use of the area was started 5 years later [1]. Early on, a rapid pressure draw down was noticed in the field and discussion about reinjecting fluid back into the system started [2]. A couple of reinjection and tracer tests were done in the early 1980's to test the field's reaction to injection. The tests in the early 1980's showed that injection into well SV-12 would provide pressure support to the system and reduce drawdown. However, due to its proximity to production wells, a rapid cooling in production wells would be expected in the field, and the well was deemed too close to the production zone to serve as an injection well. Between 1988 and 2000, injection, mostly of experimental nature, were performed into wells SV-5 and SV-6. Like SV-12, these wells were located within the production zone causing a high risk of a premature cold front in production wells. In 1998 well SV-17 was drilled about 2.4 km WSW of the production zone with the main purpose to serve as an injection well. In 2001 injection started slowly at a rate of about 24 kg/s, but in 2014 the injection rate reached an all time maximum of 190 kg/s [3]. In late 2008 well SV-24 was added as a second injection well and currently HS Orka is reinjecting about 60% of the fluid that is being extracted from the field back into the system [4], [5],[6]. In addition to the reinjection by HS Orka, 100 kg/s of cold water was flowing into the system through a feed point at about 350 m depth in well SV-24 between 2008-2010 [7]. Measurements have shown that the increased reinjection has provided a noticeable pressure support to the system. Pressure remained relatively constant from 2002 to 2008. In early 2008, energy plant VI, a 30 MW steam turbine, went into operation and despite the additional reinjection into SV-24 a pressure drawdown of 1 bar/year has been noted in the field since 2010 [8], [9].

The connections between the present injection wells and the production wells have never been studied, and possible effects due to the injection are still unknown. Tracer tests have long been used in hydrological systems, including geothermal fields, to study flow patterns and connections between wells. An important factor of geothermal field operation is proper management of reinjection. A cold front due to reinjection can cause large damage to a field, while on the other hand, large scale production where recharge is less than production can cause a rapid pressure decline in the field. In order to gain a better understanding of the system, HS Orka initiated a series of tracer tests in the summer of 2015. These tracer tests will be used to analyze connections between production wells and injection wells, predict long term cooling in the field due to current reinjection, and estimate cooling due to higher and lower injection rates.

1.1 Aim and objectives

In this paper I aim to answer a few questions that can help improve the management of the Svartsengi geothermal field and I will make recommendations on which parts of this tracer test could have been performed in a better way.
The Svartsengi geothermal field has been managed successfully without major decline in production up to this day but more knowledge can lead to even longer lifetime of the system and increased power generation. Quantitatively I will analyze the tracer test data, using a modeling method described by Axelson et al.[10], and determine whether reinjection can be continued at this rate or higher in wells SV-17 and SV-24 for the foreseeable future without significant cooling in the field. Cooling predictions for the current production and reinjection scheme will be made along with cooling predictions for higher and lower injection rates. The connections between production wells and reinjection wells have a large effect on the risk of cooling. For example, a short circuit between a reinjection well and a production well increases the risk of a premature cold front drastically, but an injection well located couple of km away from the production field is less likely to have a great affect on the temperature of production wells. Thus, I will analyze the connections based on the tracer test data and obtain flow channel parameters that are then used for cooling predictions. At the same time, it is important to gather information about the success of the tracer test itself so later tests can be improved upon. I will determine whether the optimal amount of tracer was injected into the system and whether the sampling schedule was adequate.

The results from the tests can then later be used to determine whether reinjection can be increased into wells SV-17 and SV-24 or whether the rate of reinjection needs to be reduced in order to avoid damaging the field in the long run. It may, also give information about the direction of flow in the field and how the fluid moves through it. This would, provide more information that can be used in future decision making for the field. Such as, where to add other production wells, optimization of injection well placement, and how connected the Eldvörp field is to the Svartsengi production area and the two current injection wells.

Chapter 2

Background

2.1 Tracer tests

The first large scale geothermal reinjection test was started in 1970 in the Ahuachapán geothermal field in El Salvador to test its viability of being used as a waste water disposal method [11]. Although the idea that injection could enhance energy recovery and provide pressure support for the system was recognized early on, injection was in most cases merely looked at as a means of waste water disposal with added costs [12] and [13]. However, this outlook has changed drastically and now injection is considered an essential part of sustainable and environmentally friendly management of geothermal fields. A proper injection strategy is vital to avoid negative effects such as thermal breakthrough and scaling in surface equipment and injection wells [13]. Considerable thought and research has to be put into where the most suitable location for the injection well is for a particular field because an injection well located close to the center of the reservoir will give the best pressure support, but by the same token it will maximize the risk of thermal breakthrough [10]. Once reinjection has started, the research needs to continue so the long term effects of the injection can be determined. That is done by performing a tracer test, or a set of tracer tests, in the field. Tracer tests have been used extensively in geothermal fields but the quantitative analysis of the data has been lacking in the past. If tracer test data is used to its full extent it can be used to study flow paths, quantify fluid flow in the field, and estimate long term cooling in production wells [10].

Tracer testing is an indirect method for characterizing the subsurface of hydrological systems. The success of the tracer test depends on the planning that goes into it before execution. The factors that need to be determined ahead of time include: which tracer to inject, the amount of tracer, and a rough sampling schedule [10], [14].

The selection of tracer depends on factors such as: the reservoir characteristics, background concentration, and expected recovery time. The selected tracer should ideally not be present in the system but very low constant concentrations are acceptable and can be corrected for. The tracer should not react with the reservoir rock or be absorbed, and preferably it should be easy to analyze [10]. The selected tracer needs to be stable at the reservoir temperature or have a well-characterized degradation at the reservoir conditions [14]. Once a suitable tracer has been selected the amount of tracer to inject has to be determined. The quantity of tracer to inject can be complicated to determine but a rough estimate can be obtained by performing a mass balance on the system that takes into account the injection rate, production rate and an expected recovery time [10]. Sometimes the amount of injected

tracer is based on experience from earlier tracer tests in the area. Another factor that has to be taken into account is the tracer's detection limit but typically the tracer concentration should reach at least 5-10 times the detection limit [10].

Prior to tracer injection there should be a rough sampling schedule in place but as the test progresses modifications should be made if need be. The sampling schedule should include frequency and sampling points. Sampling schedules depend on reservoir conditions and distances involved but as a general rule the sampling frequency should be very high at first and can be reduced as the test progresses [10]. Not all samples need to be analyzed but they should be kept in storage so they can be analyzed later if need be.

The transport of tracers in geothermal systems can be described by the theory of solute transport in porous and fractured underground hydrological systems [10]. The theory of solute transport has been the subject of a large number of textbooks over the years [15], [16], [17], but a comprehensive summary of tracer movement through a porous and fractured geothermal system was given by Axelsson er al. [10].

The concentration distribution of the tracer as it moves through the porous media is affected by three main mechanisms. Those are: average velocity of the fluid, variations in actual fluid particle velocities, and flux of tracer particles from regions of higher tracer concentrations to those of lower ones [15], [10]. These mechanisms are generally called advection, mechanical dispersion and finally molecular diffusion. Where advection refers to transport of particles with the average velocity of the fluid, mechanical dispersion refers to mixing of particles due to variations in actual fluid particle velocities, and molecular diffusion refers to the flux of tracer particles from regions of higher tracer concentrations to those of lower concentration. Due to the complex interaction of the different modes of transport, tracer test analysis and interpretation becomes a difficult process.

The mass flow rate of tracer through the system in the x direction is described by equation 2.1:

$$F_x = F_{x,advection} + F_{x,dispersion} \tag{2.1}$$

where F_x is in the units of kg/m^{2}s. The mass flow rate due to advection is further described by 2.2

$$F_{x,advection} = u_x \phi C \tag{2.2}$$

where u_x is the average fluid particle velocity in m/s, ϕ is the unitless porosity and C is the tracer concentration in kg/m^3.
The mass flow rate due to mechanical dispersion is represented by Fick's law:

$$F_{x,dispersion} = -\phi D_x \frac{\partial C}{\partial x} \tag{2.3}$$

where D_x is the dispersion coefficient in m^2/s, further described by:

$$D_x = \alpha_x u_x + D^* \tag{2.4}$$

where α_x is the dispersivity of the material in meters and D^* is the coefficient of molecular diffusion in m^2/s.

The differential equation for tracer transport is derived by combining the above flow equations, in the x, y and z directions (comparable equations apply for equations 2.1-2.4 in

all directions), and incorporating the conservation of mass of the tracer. For a homogeneous, isotropic and saturated medium the differential equation becomes:

$$\frac{\partial}{\partial x}[D_x\frac{\partial C}{\partial x}] + \frac{\partial}{\partial y}[D_y\frac{\partial C}{\partial y}] + \frac{\partial}{\partial z}[D_z\frac{\partial C}{\partial z}] - \frac{\partial}{\partial x}[u_x C] - \frac{\partial}{\partial y}[u_y C] - \frac{\partial}{\partial z}[u_z C] = \frac{\partial C}{\partial t} \quad (2.5)$$

In order to fully define the model appropriate boundary conditions and initial conditions need determined. The solution to such a model can often become very complicated but theoretically a mathematical solution exists for all models [10], [18]. Due to the complex nature of such detailed models, simplifying assumptions are often made in order to obtain a more simple analytical solution. An example is the one dimensional flow-channel model that will be used and discussed in further detail in section 3.3. The one dimensional flow channel model has been used successfully in numerous fields around the world in estimating flow channels between wells and predicting cooling in production wells due to reinjection.

2.2 The geological setting of Svartsengi

In order to do a thorough tracer test analysis one must have a good knowledge of the geological features of the geothermal field. One way to gain a good understanding of a geothermal field is to study current and past conceptual models of the field. The focus of this section will be on describing the current conceptual model of Svartsengi and listing previous versions of the model.

Svartsengi is located on the Reykjanes peninsula which is a unique part of the Mid-Atlantic Ridge where it rises above sea level [19]. The Mid-Atlandic Ridge is a divergent plate boundary spreading at a rate of roughly 2 cm/year, with NW-SE extensional plate movement during rifting episodes that consist of eruptions and normal faulting [20],[19]. Two major fault patterns are present on the peninsula, NE-SW faults due to the extensional plate movement and N-S striking, right lateral strike-slip faults [20], [21].

Four volcanic systems have been identified on the Reykjanes peninsula; see figure 2.1. They are defined by areas of concentrated fissure swarms consisting of NE-SW striking eruptive fissures and normal faults [20].

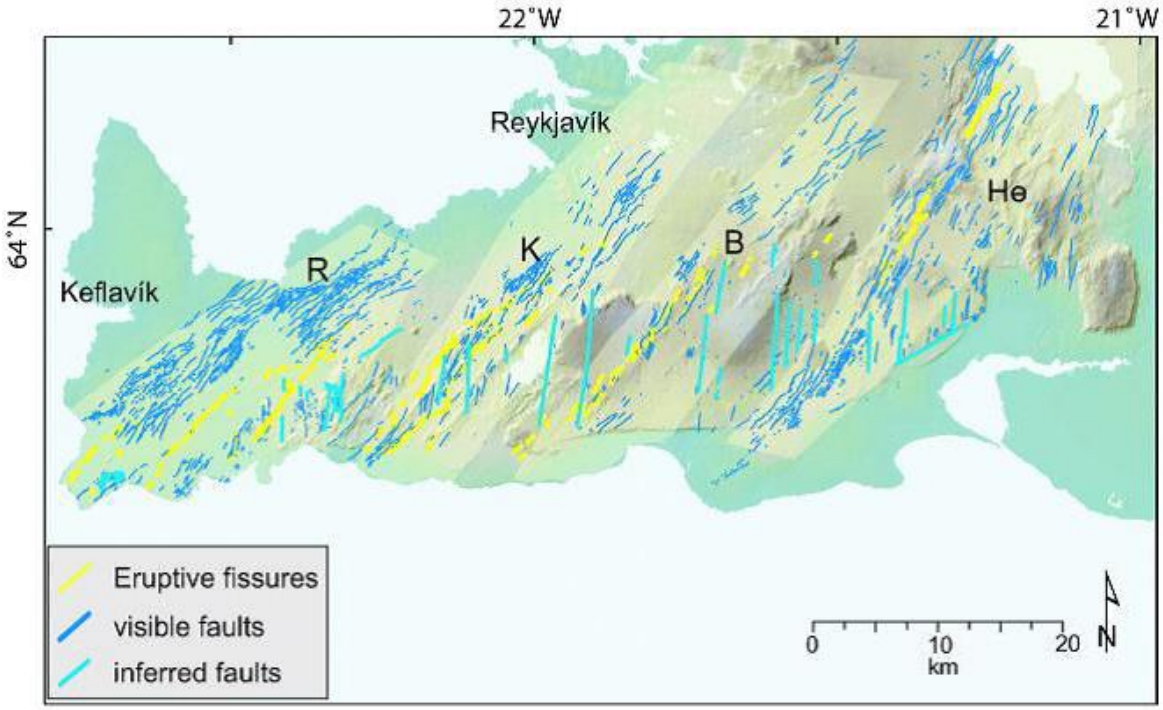

Figure 2.1: Main tectonic features at Reykjanes Peninsula. Fissure swarms from Sæmundsson (1978) shown as yellow shaded areas [19], modified from Jenness and Clifton [20].

The four volcanic systems are Reykjanes (R), Krísuvík (K), Brennisteinsfjöll (B) and Hengill (He). Reykjanes includes three high temperature geothermal fields; Svartsengi, Eldvörp and Reykjanes. Svartsengi and Eldvörp are believed to be hydrologically connected systems while Reykjanes is considered to be isolated from the two.

2.2.1 Hydrological connection between Svartsengi and Eldvörp

The proposed hydrological connection between Svartsengi and Eldvörp is supported by measurements of water level drawdown, where the drawdown in the Eldvörp observation well mirrors the drawdown at Svartsengi. On the other hand, a sharp water level drawdown in the Reykjanes field was experienced in 2006 when production was increased dramatically but the Eldvörp and Svartsengi fields were not affected [19]. More pieces of evidence supporting the theory of hydrological connection between Svartsengi and Eldvörp is a resistivity survey performed in 1981 and 1982 [22], and a resistivity cross-section from Reykjanes and Svartsengi published in 1997 [23]. Geothermal reservoirs are generally characterized by a low resistivity cap and a high resistivity core where the high temperature fluid resides. The same high resistivity core reached up to a depth of 300 meters between Svartsengi and Eldvörp. On the other hand, only a low resistivity cap was visible for 5 km at a depth of 1200 meters below sea level between Elvörp and Reykjanes, indicating far less connectivity between the two fields [23]. Simplifying assumptions and known values have been used to calculate reservoir temperatures on the Reykjanes peninsula from resistivity measurements at 600 meter below sea level [22]. The results indicated that the connection between Svartsengi and Eldvörp was much better than the one between the Reykjanes field and Eldvörp. As seen in figure 2.2, the Svartsengi and Eldvörp fields fall within the same 150°C contour, while Eldvörp and Reykjanes fall within the same 100°C contour at that same depth.

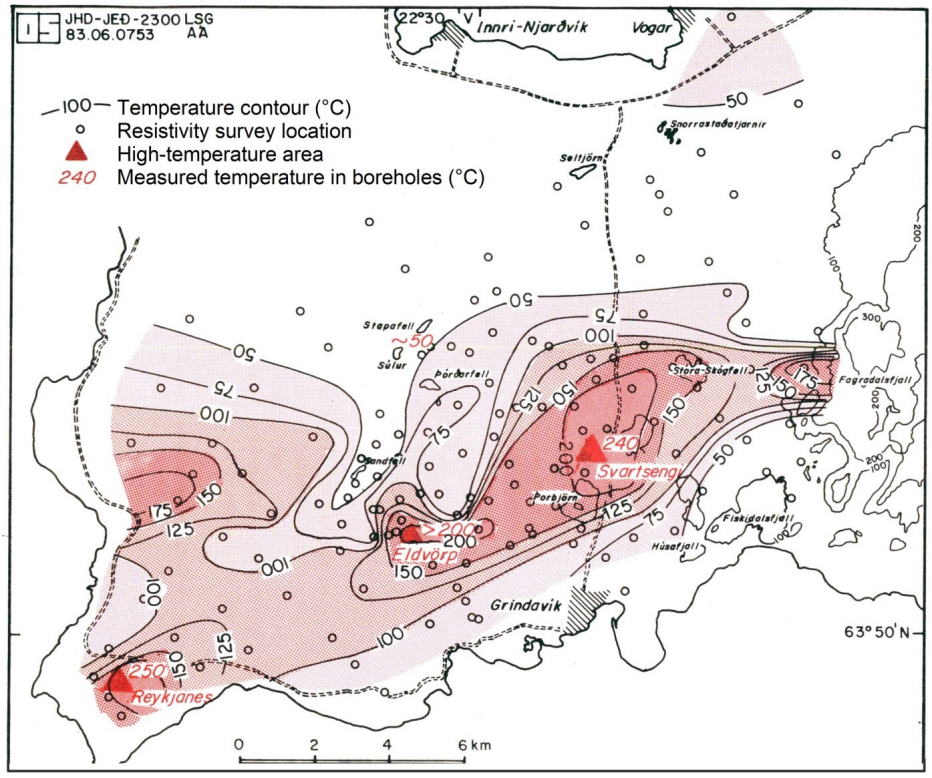

Figure 2.2: Estimated reservoir temperature at 600 meters below sea level. Modified from Gerorgsson and Tulinius [22] by Vatnaskil [19].

2.2.2 Conceptual model of Svartsengi

In the 1950's the municipalities in the Reykjanes area became interested in investigating the possibility of exploiting geothermal water for district heating purposes [19]. Research began in what is known as the Reykjanes geothermal field, but it was not until 1969 that research began in the Svartsengi field, and the first exploration well was drilled two years later [6].

The first conceptual model of Svartsengi was developed by Kjaran et al. in 1980 [24], the model was a continuation of a report done by Elíasson et al. from 1977 [25]. The model was based on data from the first three years of production along with the report from 1977. At that time only 3 wells were used for production SV-2, SV-3 and SV-4. Those three wells along with well SV-5, which was only used for observation at the time, were the basis for the initial conceptual model [24].

In 1990 Franzson presented an updated conceptual model of the Svartsengi geothermal field based on data collected over a 14 year period. At this time a number of new wells had been drilled in the field, so the new model used data from 11 wells, along with resistivity surveys and surface geological mapping [26]. Despite over a half a dozen production wells being added to the system since 1990, Franzson's model still remains the most detailed conceptual model of the field. A combined conceptual model for Svartsengi, Eldvörp and Reykjanes done by Vatnaskil consulting engineers in 2012 [19], provided a detailed summary of data from various studies and tests that have been performed in the fields over the years.

Franzson determined that the permeability of the system was largely controlled by up-flow along N-S and NNW-SSE faults and volcanic intrusions. A detailed analysis of borehole logs

by Franzson [26] showed a high concentration of intrusives at a depth range of 1100-1300 meters in wells SV-6, SV-7, SV-8 and SV-12 as seen in figure 2.3.

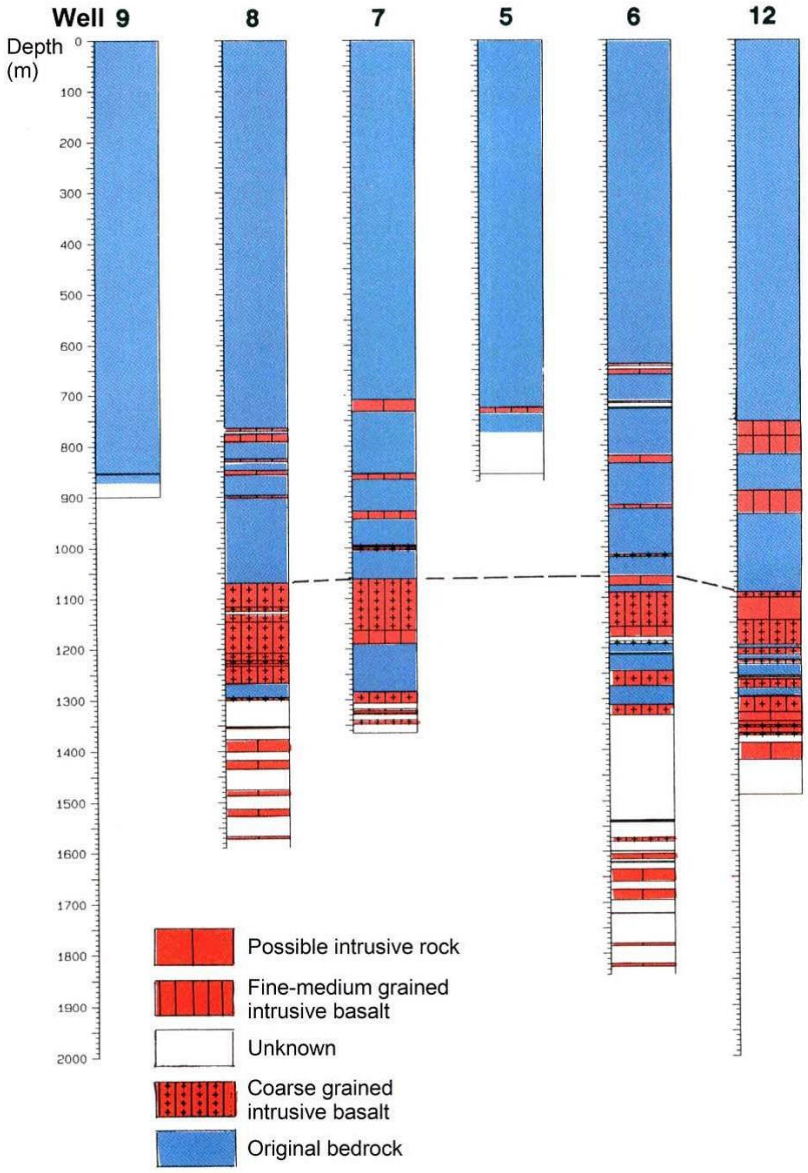

Figure 2.3: Measured volcanic intrusions, modified by Vatnaskil from Franzson [26], [19].

At this depth the portion of intrusives is 90% or greater and they lie nearly horizontal in the bedrock, as illustrated in figure 2.4. Due to the alignment of the intrusive rock a high permeability feed zone facilitates a good hydrological connection between wells at a depth range of 1100-1300 meters [26], [19]. An extensive report with a geological cross-section including wells drilled after the drilling of SV-12 does not exist, but reports for other wells can give an idea of the geology of a larger section of Svartsengi.

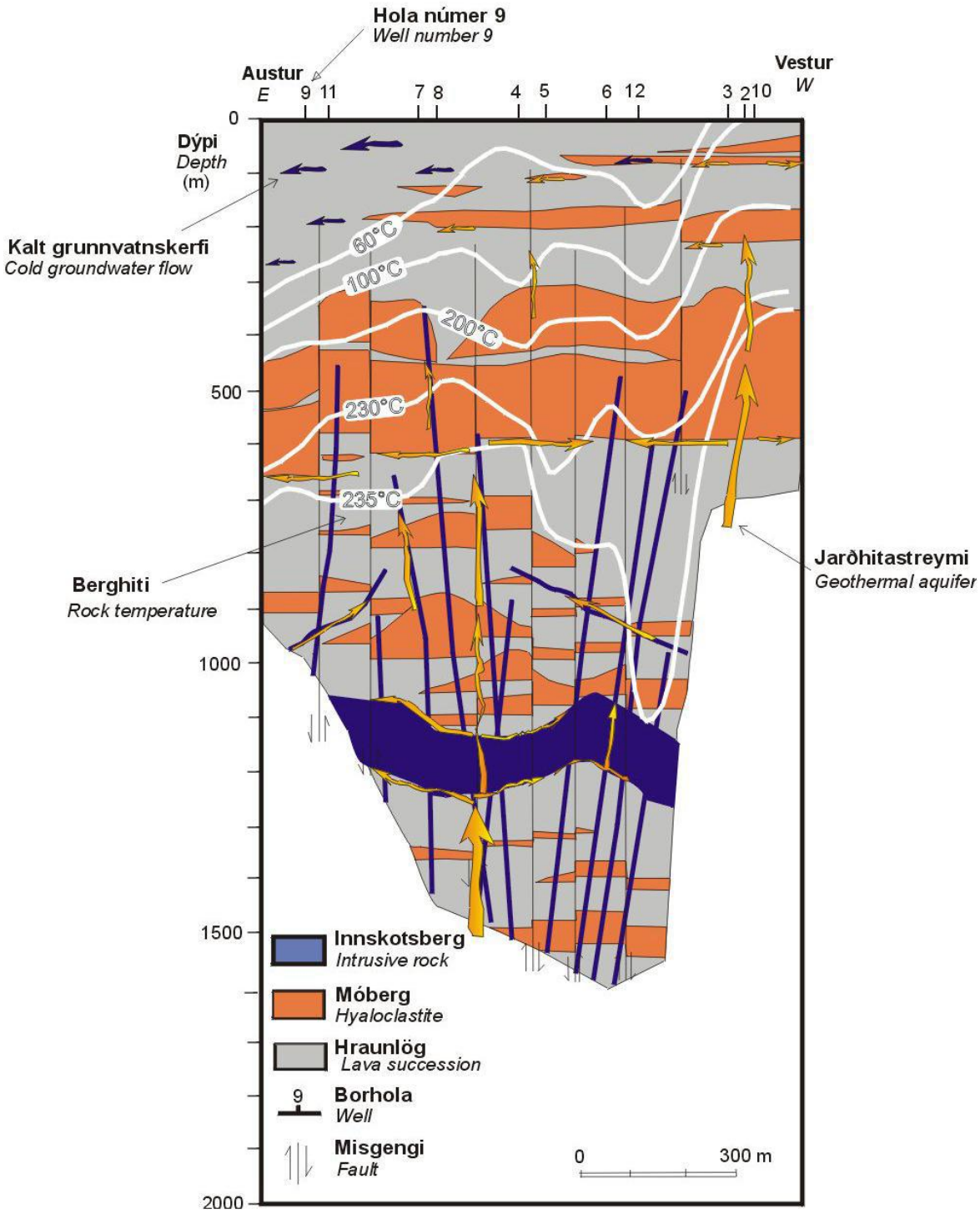

Figure 2.4: Geologic cross-section at Svartsengi showing sequence of lava and hyaloclastite layers, intrusive rock, faults and proposed flow patterns within geothermal and groundwater aquifers. Modified by Vatnaskil from Franzson [19], [26].

SV-14 is located 45 m SE of well SV-10. Drill cuttings indicate that the well is located near the SE boundary of the steam zone and feed points were located at horizontal boundaries between lava and hyaloclastite layers [27]. An examination of data obtained during the drilling of SV-14 also showed that geological layers in well SV-14 corresponded to layers observed in SV-10, SV-3 and SV-2 and there are no major normal faults in the area [27]. Surface and geological data from wells located in the steam zone show that it is likely steam up-flow could be traced to a N-S fault cutting through the zone and several NE-SW faults

cutting the N-S fault, shown in figure 2.5. The crossing of these faults are the sources of steam up-flow from the geothermal reservoir, and horizontal boundaries spread the up-flow to the wells.

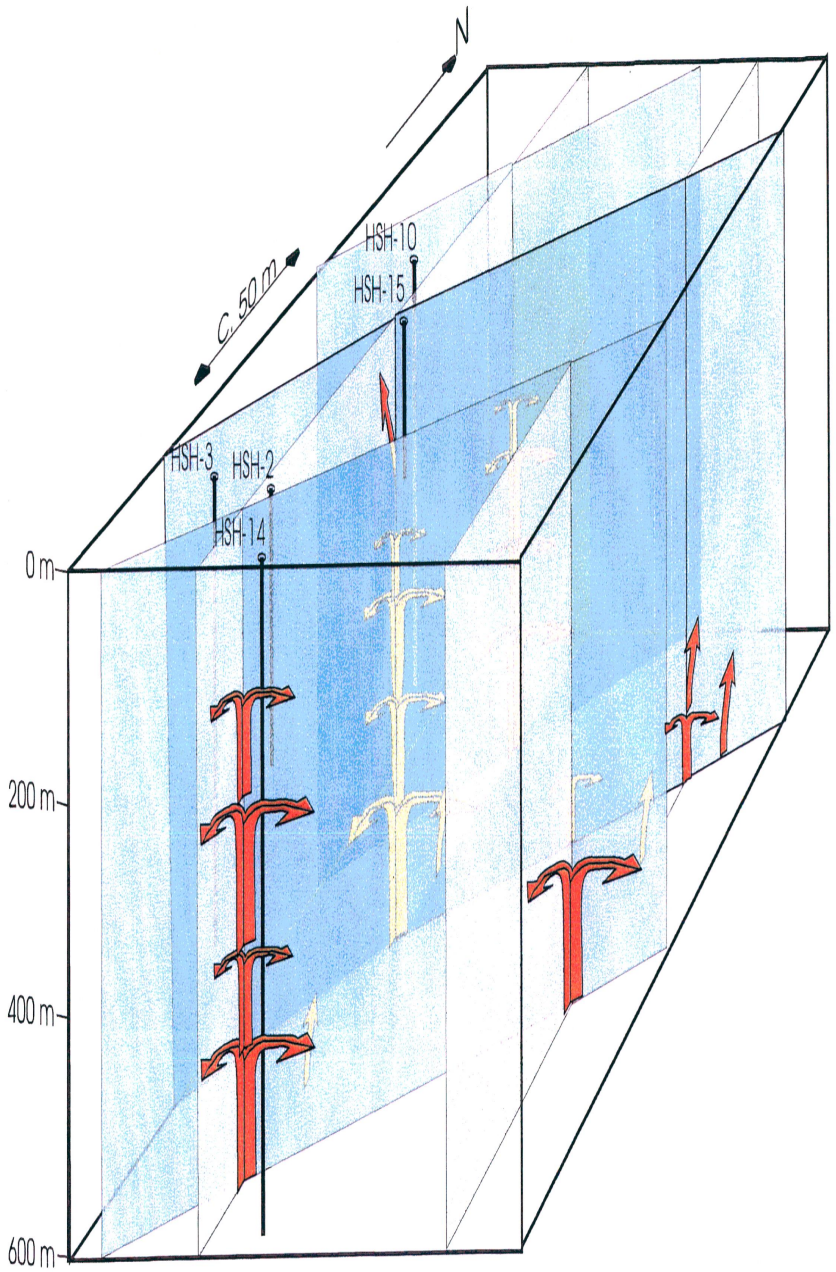

Figure 2.5: A possible model of the steam zone at Svartsengi [27].

SV-18 is located 250 meters SSE of well SV-8. The well was drilled as a so called step-out well to test the boundaries of the geothermal system. It was believed that the hot up-flow of the system follows a N-S trend and the drilling of SV-18 was a part of exploring whether this zone was closer to the heat source than other areas. Data obtained during the drilling of the well showed that the geological cross-section in well SV-18 was comparable to other wells at Svartsengi, but most of the layers started 30-50 m lower than in other wells. The only major

structure that was absent was a dolerite intrusive belt located at 1100-1300 meters in other wells (see figure 2.4)[28]. Geological data showed that the formation temperature around the well was higher than around wells to the north and high temperature formations extend about 100 meter higher than in other wells [28]. This evidence supports the theory that SV-18 is located closer to the hot up-flow than other wells. However, the current temperature in the well is only 240°C, similar to the average temperature in the geothermal field.

Little data on the geology of SV-19 has been published but a geological cross-section based on drill cuttings was compared to figure 2.4 as seen in figure 2.6 [28]. SV-19 is located about 80 m east of SV-8 and 150 m south of well SV-5, see figure 2.7. The cross-section of SV-19 fully supports the earlier cross-section created from the wells drilled in the early history of Svartsengi. No major discrepancies are noted, hyaloclastite layers at 400m and 550m depth fall right into formations noted earlier and the horizontal layer of intrusives at 1100-1200m depth is evident in SV-19.

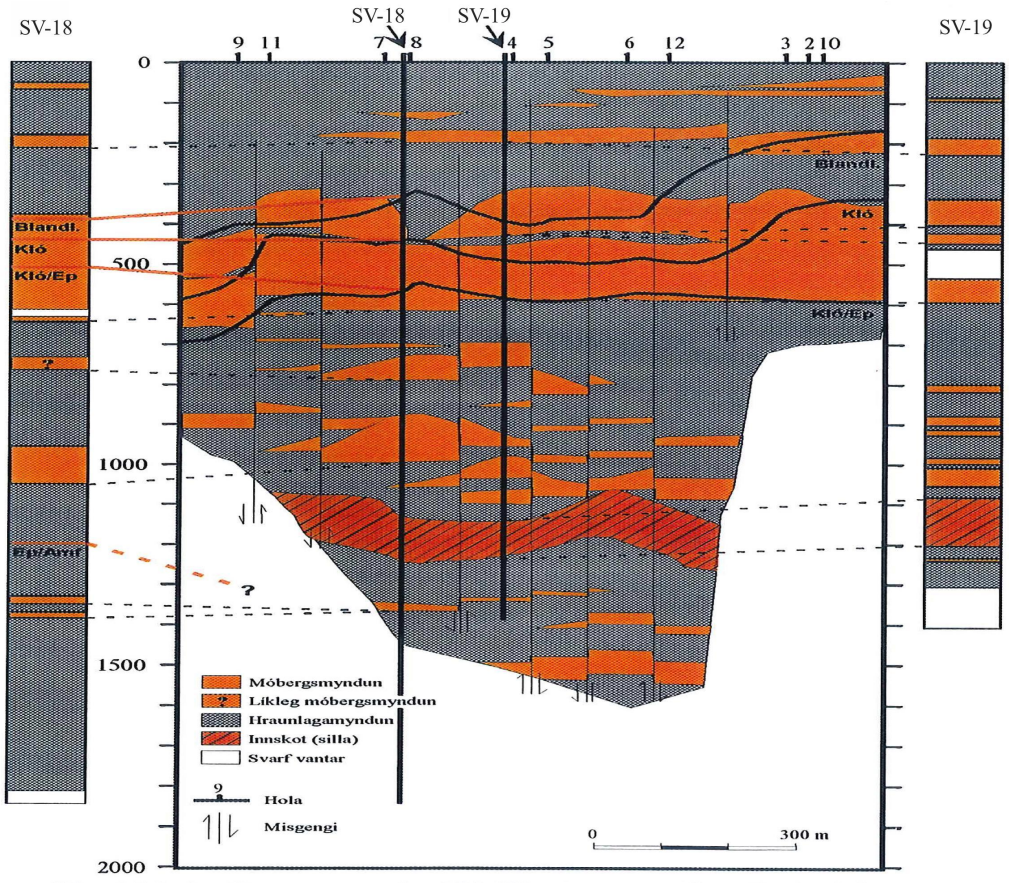

Figure 2.6: A comparison of geological cross-section in wells SV-18 and SV-19 to figure 2.4 [28].

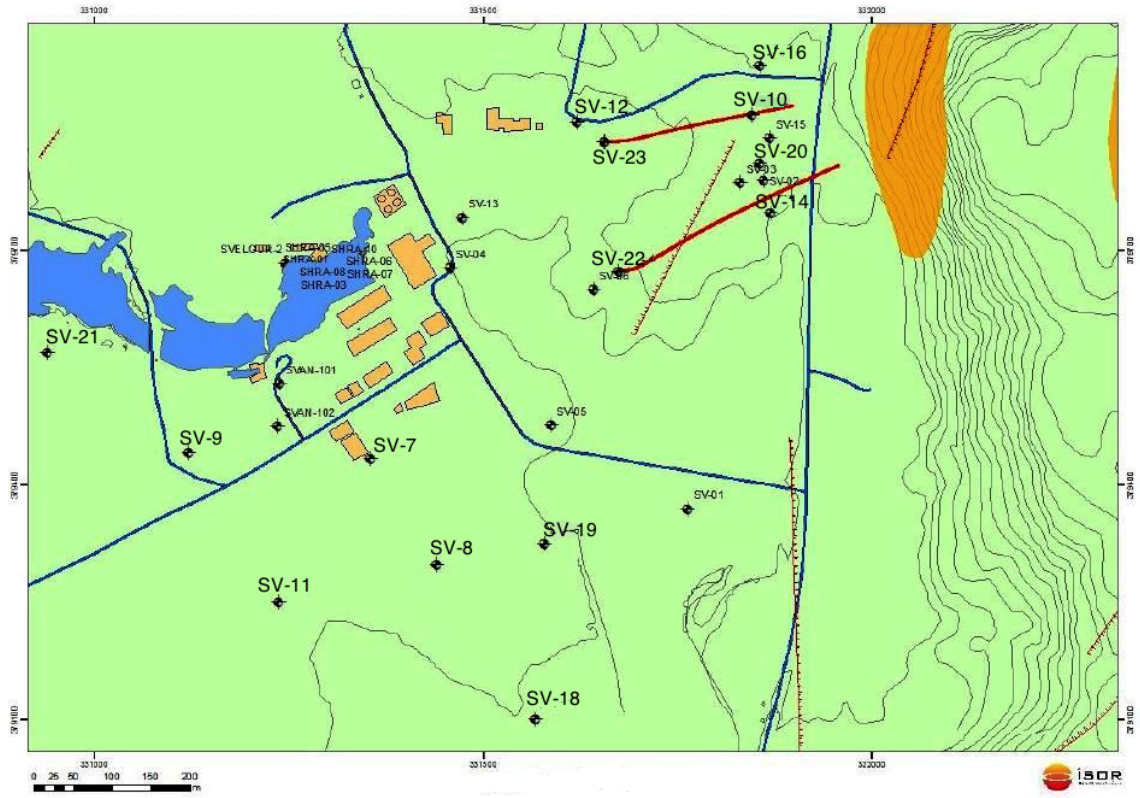

Figure 2.7: Location of production wells at Svartsengi, direction of directionally drilled wells shown in red. Modified from [7].

SV-17 was drilled specifically as an injection well. The well is located 2.4 km WSW of the main production zone but resistivity measurements indicated that high temperatures could be found at shallow depth in the area. The temperature of the well was measured to be 240°C and capable of serving either as a production well or an injection well. Despite the distance from main production zone geological layers could be traced back to the same origin of those of the production wells at Svartsengi, but the high temperature zone is believed to be positioned 100-200 m lower than in other wells [29]. Feed points in the well are connected with two vertical basalt intrusions at a depth between 450-700 m, where a large number of relatively small feed points were noted. Horizontal fractures near the bottom of the well correspond the two largest feed points in the well [29].

SV-24 was drilled within the same well platform as SV-17, like SV-17 it was intended as an injection well right from the start. SV-24 is a directionally drilled well with a drilled length of 1098 meters. Original plans had intended the well to be 2000 m deep but a high injectivity index of 35 l/s/bar at 1000 m depth indicated a high permeability in the well and there was no need to drill deeper. Main feed points in the well were noted at 649m and 674m [30].

The geologic cross-section in figure 2.4 and information from more recent boreholes show a sequence of lava flows separated by hyaloclastite layers. The hyaloclastite layers are generally far less permeable than the lava layers, and therefore hinder the flow of fluid [19]. The thick layer of hyaloclastite at 300 to 600 meters depth is likely to act as a caprock, separating the geothermal reservoir from a shallow groundwater aquifer sitting on top. The caprock is fractured on the NE side of the reservoir, allowing up flow of geothermal fluid that

gives rise to the creation of a natural steam zone around wells SV-2, SV-3, SV-10, SV-14, SV-16 and SV-20 [26]. Local decrease in reservoir pressure due to production has caused the natural steam zone to expand. The enlargement of the original steam zone caused wells SV-7 and SV-11 to start producing both from the liquid dominated reservoir and the steam zone [31].

Later on in this study, when analysis of the tracer data is performed, parameters such as distance between injection and production wells, depth of wells, casing depth, and feed points are used to evaluate tracer recovery and gain a further insight into the characteristics of the geothermal system. Detailed information about well and casing depths in the geothermal systems at Svartsengi and Eldvörp were presented in [7]. Beneath the casing either a slotted liner or no liner has been inserted for the production portion of the wells and geothermal fluid can easily flow into the wells from various feed points. A summary of well feed points was created using available borehole logs and Franzson's summary [26], [27], [28], [32], [33], [29], [30], [34]. Unfortunately, borehole logs or information about feed points was not available for all wells. Presented in table 2.1 is all data available from the sources mentioned above. In addition, distances between wells were measured using Petrel [35], where distances to and from directionally drilled wells were measured at the top of the wells. Note that this list does not present all feed points encountered during drilling, but only those that were considered likely to be large contributors to production from the wells. Note that, in general, the casing of steam zone wells is considerably shallower than those of two phase or liquid phase wells. The exception here is well SV-23, a steam phase only well, where the casing reaches down to 489 m. The reason behind that being that SV-23 is a directionally drilled well; where the well head is located outside the original steam zone but drilled directionally into it.

The initial conceptual model proposed a trough shaped highly permeable 2 km^2 reservoir, opposed to 6-8 km^2 estimated by [23] and [22], with relatively impermeable boundaries on three sides [24].This hypothesis has since been supported by numerous land subsidence measurements [36], [37]. The subsidence data presented in figure 2.8 provides a detailed summary of data collected between 1967 and 1999. The data supports the original hypothesis and subsidence contours, extending from Svartsengi towards Eldvörp in the SW direction, showcase the hydrological connection between Svartsengi and Eldvörp. The short distance between contours east of Svartsengi show a rapid decline in subsidence rate, suggesting geological formations that limit permeability in that direction [19]. Earthquake epicenters on the Reykjanes peninsula have been thoroughly studied through the years. The epicenters form a belt on the the peninsula that cuts through the Reykjanes geothermal field, Eldvörp and Svartsengi. Both Svartsegni and Eldvörp are located in the middle of the belt, as seen in figure 2.9. Earthquakes make way for cracks and fractures, consequently increasing the permeability of the rock matrix. The outside boundaries of the earthquake belt are therefore likely to form boundaries of lower permeability around the reservoir in the north and south direction. This is supported by closeness of subsidence contours north and south of the Svartsengi. The land subsidence data not only gives an idea of the shape of the reservoir, it also provides information on the area geothermal fluid is being extracted from at depth and the relative lateral extent of the reservoir [19]. About 100 km^2 of land area around Svartsengi has been affected by subsidence due to production, which is a much larger area than the production zone itself [19],[37].

Table 2.1: Information about well depth and distances from reinjection wells.

Well	Depth [m]	Casing [m]	Feed points [m]	Distance from [m]	
				SV-24	SV-17
SV-7	1438	600	1350	2626	2598
SV-8	1603.5	622		2640	2612
SV-9	994	588	441, 907	2431	2401
SV-10	425	220		3274	3244
SV-11	1141	582		2436	2409
SV-14	612.4	195	349-350	3230	3201
SV-16	440	246		3316	3287
SV-18	1845	770	735, 1815	2677	2651
SV-19	1600	715		2776	2748
SV-20	430.5	245	244-256,350, 404	3250	3221
SV-21	1475	844		2354	2323
SV-22	862	386	388, 410, 510-515, 620-640	3023	2994
SV-23	698	489	608, 646	3096	3066
EG-2	1265	520		2739	2761
SV-17	1260	789	1052, 1125, 1220	—	—
SV-24	1086	300	649, 674	—	—

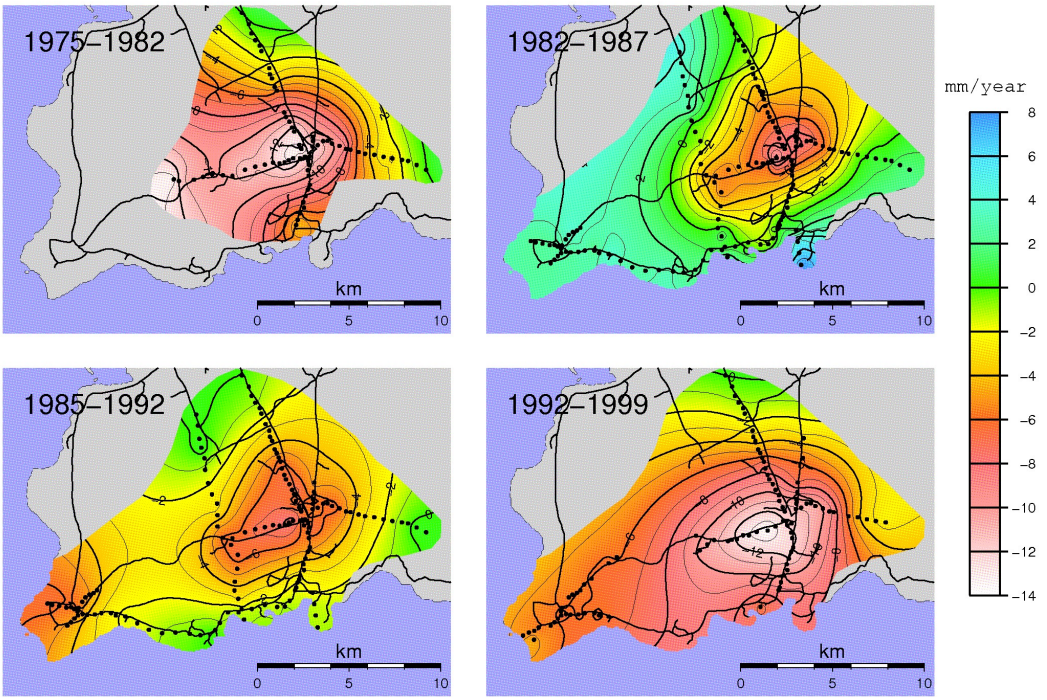

Figure 2.8: Subsidence rate at the outer part of the Reykjanes peninsula for four time intervals. Bench marks are shown by solid circles, roads are shown by thick lines, contour intervals are 1 mm/year [37].

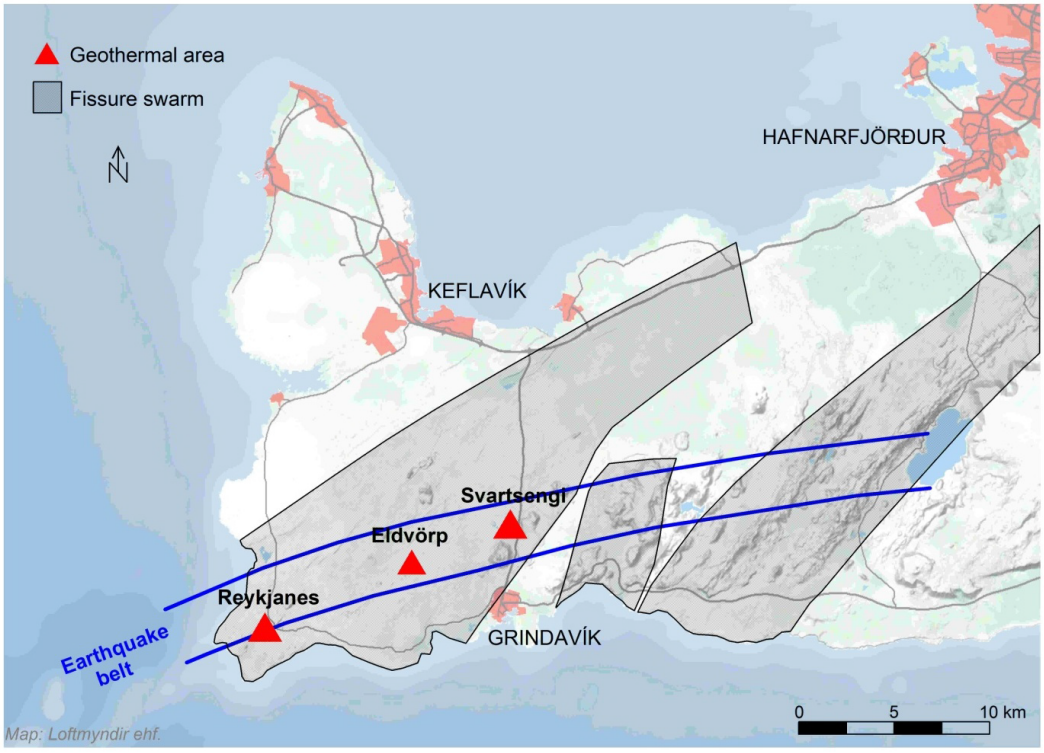

Figure 2.9: Location of main fussure swarms and earthquake belt on Reykjanes peninsula, modified from Kjaran et al., 1980 [19], [24].

2.3 The injection history of Svartstengi

Early on discussion started whether or not it would benefit the Svartsengi geothermal field to inject some of the production fluid into the field again. This came about after considerable drawdown in the field was recorded in 1976 [2].
In march 1982 the first injection well, SV-12, was drilled. It was drilled with the following criteria in mind [2]:

1. It was within the known reservoir.

2. It should have the potential to be used as a production well if injection was not feasible.

The well is located in the north end of the current production zone, about 200 m west of SV-10. Before the injection test started it was proposed that brine would be injected for a week into the reservoir, then hot fresh water for a week and then finally brine for 4-8 weeks. However, little was known about the effect of injecting brine into the reservoir, and at the time changes were being made to the power plant so the supply of hot fresh water was limited. Thus the test was performed using cold water, which had the advantage of being in ample supply but the disadvantages of larger temperature difference and higher risk of corrosion [38].

This first injection test lasted 24 days but during that time 63-65 l/s of cold water were injected into SV-12. The water level in SV-4 was monitored during the test along with the water level in SV-12. The water level in SV-12 rose as soon as the tests started and about a week after the injection stared a considerable increase was noted in SV-4. Along with the increased water level there was an increase in the amount of gas in SV-4 which caused the water level monitor to fail. About three weeks after injection had been terminated the water level had fallen approximately 100 m. This first test showed that an injection into SV-12 would provide a pressure support for the system and reduce drawdown. However, a simultaneous tracer test showed that the well might be located too close to the production field. The results from the tracer test will be discussed in further detail in a later section[38].

Following recommendations that were provided as a result of the injection test in 1982, another more extensive test was performed in 1984. Again the test was twofold, an injection test and simultaneous tracer tests. The supersaturation of the spent geothermal brine was a cause for concern about silica deposits in the injection well and pipelines. One of the purposes of this test was to see whether mixing condensate with the brine would allow the brine to be injected without considerable silica deposits before reaching the reservoir. The test was done with a 20% condensate and 80% brine mixture at a flow rate of 50 l/s and lasted 77 days. Again the water level in SV-4 showed a direct correlation to the amount that was being injected into the system, or in other words the total amount of fluid extracted from the reservoir. However, the injection did not have a noticeable effect on other wells. The mixing of 20% condensate with the brine could not be maintained because at the second half of the test the production of condensate dropped and only 10% mixing was achieved which did not turn out to be sufficient. A rapid increase in water level in SV-12 occurred and injection was stopped to avoid permanently damaging the well.

Once the injection of condensate and brine mix had stopped the injection of hot fresh water into SV-12 was continued for about 4 years. During that time the flow rate ranged from 40 kg/s to 90 kg/s. Once injection into well 12 was terminated, injection into SV-5 started and

continued for 2 years at a flow rate of 20-60 kg/s. The injection into well 5 was terminated in 1990 and no more experiments were done with injection of fluid into the system for the next three years. In 1993 injection of condensate into SV-6 was started and done on and off for the next 7 years. The injection from 1984-2000 was mostly of experimental nature and all three wells, SV-12, SV-6 and SV-5 are located within the production zone. If injection had been continued into these wells at the same flow rates, some pressure support would have been provided but a rapid cooling should have been expected in the field[1].

In 1998 the drilling of SV-17 was started. The well was intended to be an injection well and provide pressure support for the system without the risk of rapid cooling. The well is 1260 km deep and located 2.5 km WSW of the production field. Injection into the well was not started until 2001 when 30 kg/s of condensate brine mixture was injected. In 1992 and 1994 further research was done on the silica scaling problem experienced in 1984. There it was determined that 38% of the mixture had to be condensate if only 1 mm of scaling was allowed per year. If no scaling was permitted condensate had to account for 52%. Thus, the mixture injected into well SV-17 contains 40-50% condensate and 50-60% brine at a temperature of 95°C [1]. The injection was slowly increased from 30 kg/s in 2001 to 150 kg/s in 2007 [39] [3].

In late 2008 SV-24 was added as a second injection well [4]. The well was drilled on the same platform as SV-17, located about 2.3 km from the nearest production well. The injection in well SV-24 started out slow, but in 2014 the total reinjection into the field averaged about 300 kg/s, where approximately 35% of the fluid was injected in SV-24 [3]. In addition to the fluid injected by HS Orka, about 100 kg/s of cold ground water leaked into well SV-24 from 2008 until the responsible feed point was sealed off in 2010 by HS Orka [7].

Temperature measurements done following the reinjection into SV-17 and SV-24 show that temperature has not been affected by injection of the 95°C fluid. However, pressure data show a good pressure support resulting from the injection in monitoring wells as illustrated in figure 2.10.

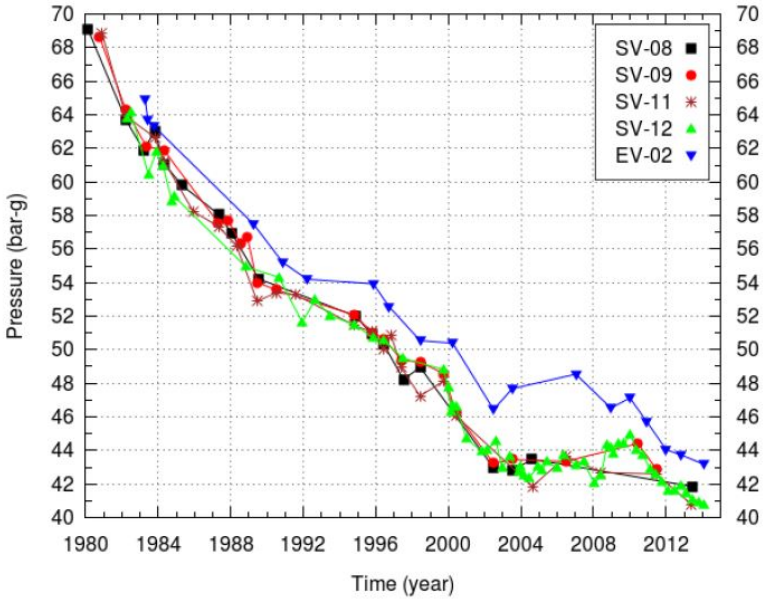

Figure 2.10: Pressure at 900 m depth in Svartsengi and Eldvörp from 1980-2013 [7].

The pressure data from Svartsengi and Eldvörp show a strong correlation between the operation of the power plant and well pressure fluctuations. In November 1999 Energy Plant V started producing electricity [40]. Shortly after, in 2000, the field pressure started dropping at an increased rate. But in 2002, once injection into SV-17 had reached about 55 kg/s, pressure started stabilizing and stayed almost constant until early 2008 [3],[7]. In early 2008 Energy Plant VI was commissioned and pressure started decreasing again [7]. However, the new trend did not last; by the end of 2008 the pressure started increasing again due to reinjection into SV-24. Since 2010 the pressure has been decreasing at a rate about 1.1 bar/year due to the increased production intensity in 2008. The reason for the late arrival of pressure decrease can likely be traced in some part back to the inflow of cold fluid into SV-24 that was sealed off in 2010.

2.4 Tracer tests in the Svartsengi geothermal field

As previously stated, two combined injection and tracer tests were performed in the early 1980s. The objectives and results of the injection tests were discussed in detail in the previous section. The focus in this section will be on the purpose and results of the tracer tests.

The test performed in 1982 was the first tracer test in a high temperature field in Iceland, and due to lack of experience Hitaveita Sudurnesja decided to perform a simple test to begin with[2]. Cold fresh water was injected into well SV-12. Sodium concentration in the geothermal brine and nitrogen ratio in the gas coming from production wells were used as tracers. The test was performed as described below [38]:

1. Cold fresh water at a flow rate of 63-65 l/s was injected into the newly drilled injection well, SV-12, for 24 days.

2. Brine samples were collected from the separators of wells 6-11 every 2 hours for 11 weeks. Sampling was terminated after 70 days.

3. The concentration of sodium in the brine was analyzed. This was done to monitor the salinity of the brine. If there was a short circuit between the injection well and any of the production wells, the salinity in that particular production well should drop significantly.

4. Steam phase and gas samples were taken every week after the first two weeks to monitor the ratio of nitrogen in the gas. Carbon dioxide normally makes up about 98% of the gases that travel with the brine from the wells at Svartsengi. Fresh water contains oxygen and nitrogen and when the fresh water is injected into the reservoir those gases are mixed in with the brine. The ratio of nitrogen in the gas of wells that are affected by the in-flow of fresh water should rise compared to normal levels.Thus, the ratio of nitrogen in the gas was used to gather information about how the injected fresh water traveled through the reservoir.

Before the injection started brine samples were taken once per day for a week to get base concentration for each well. Wells SV-6, SV-9 and SV-10 all showed a change in sodium concentration, as seen in figure 2.11. Well SV-10 was the first to respond, 55 minutes after injection started the sodium concentration in the well dropped from 7500 ppm to 4500 ppm. After three hours the concentration had returned to normal. A drop in concentration and a return to normal levels was observed two more times during the test period. Well

SV-9 showed a drop in sodium concentration of 6000 ppm 34 days after injection and 3 days later the concentration had returned to normal values. Well 6 also showed a change in sodium concentration but the well had been shut in before the test and then again for 2 hours during the test while the well was connected to the power plant. For the first week of the test the well was discharged through a silencer. The changes in boiling and well condition thus made it hard to interpret the data. Wells SV-7, SV-8 and SV-11 did not show a significant sodium concentration during the test. Similarly, wells 6 and SV-10 shows the largest increase in nitrogen ratio in the gas samples. Wells SV-8, SV-9 and SV-11 do show a response but considerably less than wells SV-6 and SV-10. as seen in figure 2.12 [38].

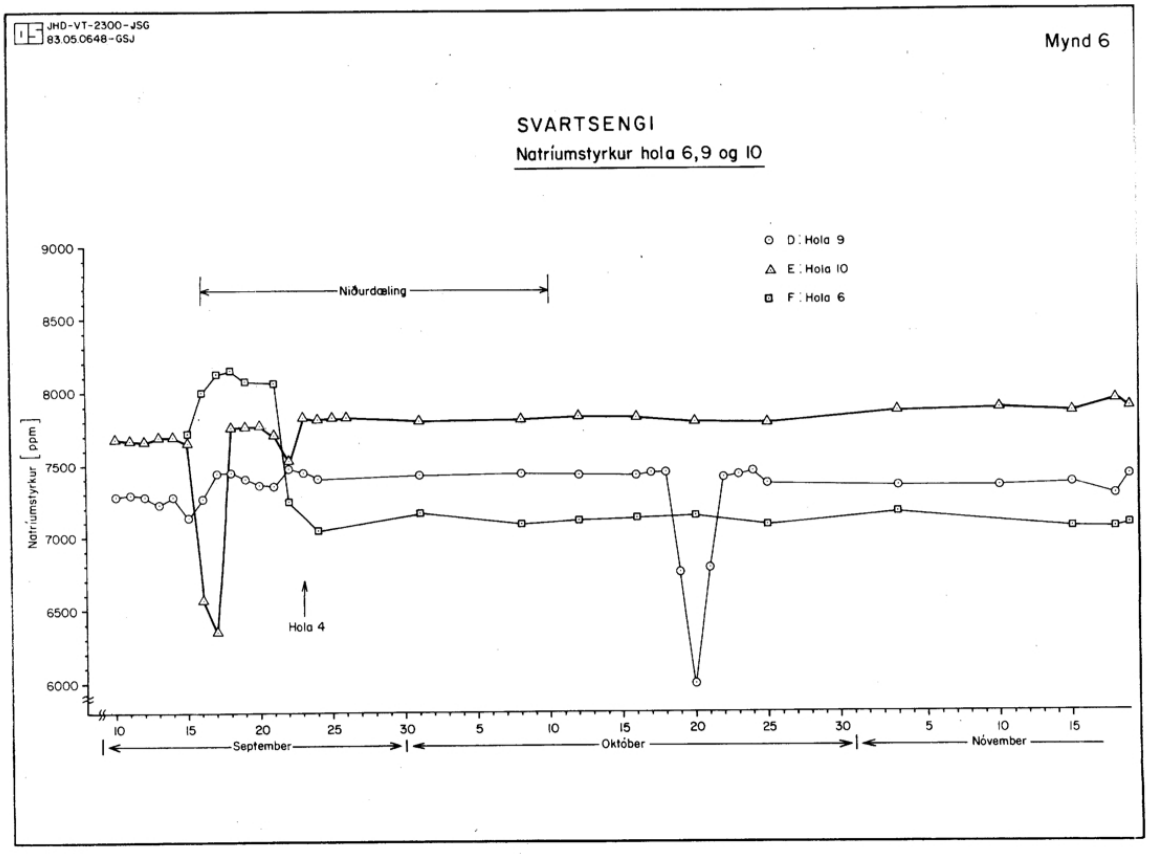

Figure 2.11: Sodium concentration in well SV-6, SV-9 and SV-10 [38].

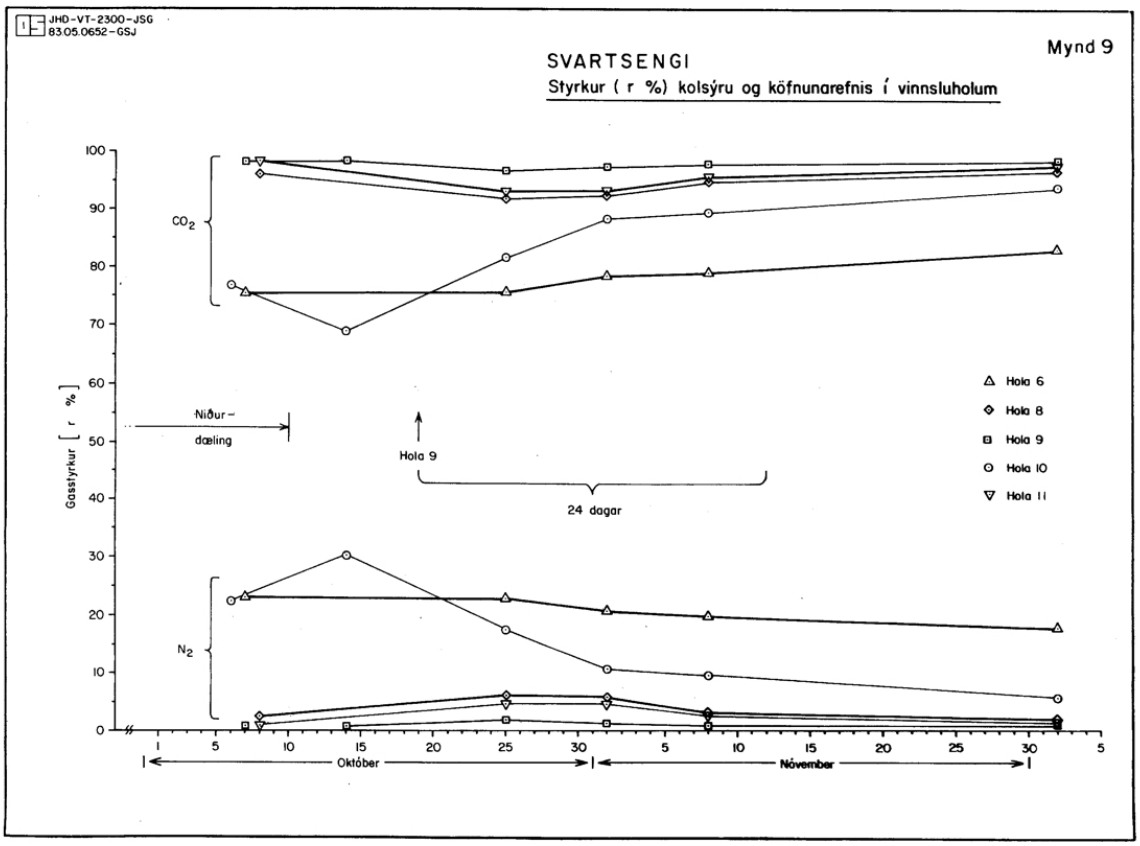

Figure 2.12: Percentage of carbondioxide and nitrogen in gas in wells SV-6, SV-8, SV-9, SV-10 and SV-11 [38].

The main results from this first tracer test in a high temperature field in Iceland were that well 12 was too close to the production field to be used as an injection well. The short response time indicated that there was a very strong connection between well SV-10 and SV-12 and long term injection would most likely cause cooling in the field, and possibly very rapidly. At this point further testing of the well was recommended [38].

In 1984 the second tracer test was performed at Svartsengi, based on guidelines from the previous test. Again the test was performed in conjunction with an injection test in well 12, the injection test which was discussed in the previous section. This time two tracers were injected into the field, iodide and Rhodamine WT. The tracers were chosen according to the guidelines outlined in background section about tracer tests. However, iodide did have a background concentration of 177 ppb [41]. The main purpose of using Rhodamine WT along with the iodide was to test its stability in a high temperature reservoir, the Rhodamine WT had been used successfully in low temperature fields but had not been tested in high temperature fields.

On July 26th 37 liters of Rhodamine WT mixed with few a hundred liters of injection fluid were injected into well SV-12. The day after 350 liters of potassium iodide dissolved in a few hundred liters of injection fluid were injected. The sampling frequency for this second test was much higher than of the first test to begin with. At first samples were collected every hour, but quickly decreased to 12, 6, 4 and then finally 2 samples per day. The first sign of iodide occurred 40 hours after injection in well SV-6 and reached a peak value after 100 hours [41]. It should be noted that well SV-10, the well that had shown the strongest connection to well SV-12 in the previous test, was at this time producing solely from the

steam cap that had formed due to production, and no liquid samples could be obtained [2]. Other wells that the iodide was detected in were wells SV-7 and SV-8. However, it was estimated that only about 4% combined of the iodide injected was recovered in wells SV-7 and SV-8 while 38% were recovered in well SV-6 [41]. The Rhodamine WT experiment did not prove to be successful. The Rhodamine WT did show up in the system at the same time as the iodide and reached a peak value after 100 hours. The concentration however is much lower than would be expected based on the iodide return and drops off much faster. Thus, it was determined that the Rhodamine WT was not stable enough at such high temperatures and silica deposits in the sample interfered with the analysis. The conclusions drawn from the tracer test were that:

1. Well SV-6 is fed through a single fracture and porous rocks. This was based on the fact that three models were needed to model the high peak and long tail of the recovery curve [42].

2. Prolonged injection into well SV-12 would cause rapid cooling in well SV-6 and make it unfit for production relatively quickly [41].

3. Wells south of the injection well would be most affected, but wells placed east and west of well SV-12 would most likely not experience cooling until decades later [41].

The results from the 1982 and 1984 tracer tests were both in agreement that well SV-12 was too close to the production field to avoid cooling due to injection. The test also showed that the predominant direction of flow in the field was consistent with the direction of the fractures; north-south [41]. The wells south of the injection well had the highest and fastest recovery of tracers while wells west and east of well 12 had a much lower recovery.

No other tracer tests have been performed in the Svartsengi field until now despite continuous injection into SV-17 and SV-24. The wells are located about 2.5 km south-west of the production zone. Thus, the current test is expected to take a considerably longer time than the tests performed through SV-12 in the 1980s.

Chapter 3

Methods

The tracer test at Svartsengi began on June 23rd 2015 when 400 kg of the liquid phase tracer 2,6-napthalene disulfonate (NDS) were dissolved in 12 m^3 of water, and injected into well SV-24. The injection lasted about 20 minutes. Liquid background samples were taken on June 19th and at the end of May by Iceland GeoSurvey (ÍSOR). The first samples after tracer injection were taken on June 25th. On June 28th 86,78 kg of the steam phase tracer sulfurhexafluoride (SF_6) were injected into well SV-24. The tracer injection took 11 hours and 39 minutes. Background steam samples were taken by ÍSOR at the end of May and the first samples after injection of tracer were taken June 30th and July 1st. On July 8th 400 kg of the liquid phase tracer 2,7-NDS dissolved in approximately 12 m^3 of water were injected into well SV-17. The injection lasted 30 minutes.

The sampling schedule was designed according to general rules described in section 2.1. Both steam and liquid phase sampling schedules are presented in table 3.1

Table 3.1: Sampling schedule for both SF_6 and NDS.

Liquid phase		Steam Phase	
Week	Sampling Frequency	Week	Sampling Frequency
1	1x per week	1-2	3x per week
2-6	3x per week	3-8	2x per week
7-9	2x per week	9-14	1x per week
10>	1x per week	15-17	Every other week

The distance between the injection wells and the closest production well is about 2.3 km, see table 2.1. Thus, the chance of the liquid tracer showing up in the system within the first week were determined to be extremely low and only one sample was taken in the first week. The following five weeks the sampling frequency was increased to three times per week in case the liquid tracer traveled with high velocity through the system and a sharp peak would be experienced. After seven weeks without any signs of the liquid tracers it was determined that the chances of a sharp peak would be highly unlikely and the it was safe to reduce the sampling frequency without running the risk of losing any significant data. At this point the sampling frequency for the liquid phase was reduced down to twice per week and two weeks later down to once per week.

The steam tracer was expected to travel at a much greater speed through the system due to a much lower density and higher entropy of the gas phase than the liquid phase. Therefore, the sampling frequency for the steam phase tracers started out at three times per week to make sure all sharp peaks would be detected. Two weeks after injection the frequency was reduced down to twice a week. At this point it was determined that the SF_6 traveled at a low enough speed through the system that no important information would be lost with a reduced frequency. The steam tracer was first detected 18 days past injection in wells SV-7 and SV-11. On August 20th it was determined to reduce the sampling frequency down to once per week in the following week, week 9. At this point the concentration of SF_6 had already reached a maximum and the concentrations for each well were coming down at a steady pace close to detection limits. However, the next batch of results showed that the concentration was starting to rise again in a couple of the wells. This posed the question whether the frequency should be increased again or kept at the current rate. It was determined that given the previous pattern of tracer returns and the relatively long time past injection that a sharp peak would not be very likely and one sample per week would be sufficient. The sampling frequency of one sample per week was kept constant through September. At the end of September the concentration had dropped down to detection limits. At this point it was considered highly unlikely that the concentration would rise again and the sampling frequency was reduced down to every other week until steam sampling was terminated in week 17.

3.1 Sampling methods

3.1.1 Vapor phase sampling methods

A Giggenbach glass bottle was used for gas phase samples. 52 bottles were used for this experiment, each bottle was weighed when empty and then filled with water to calculate exact volume. Due to the number of monitoring wells and sampling frequency there was a rather quick turn around for each bottle for the first few weeks. Each bottle was cleaned thoroughly before 100 ml of 10 M NaOH solution was added to the bottle. Finally, the bottle was evacuated for 4 minutes and weighed.

The gas phase at Svartsengi consists mainly of CO_2 and H_2S. In fact CO_2 and H_2S make up about 99 mole% of the gas coming from the wells [43]. Thus, the caustic solution is added to Giggenbach bottle before sampling, acidic gases dissolve in the NaOH solution allowing the other gases to be collected in the headspace in detectable concentrations.

A Webre separator, shown in figure 3.1, was utilized at the wellhead. Each well had its own Webre separator to minimize contamination between wells.

At the start of sampling geothermal fluid from the well was allowed to flow through both vapor and fluid vent with a full opening to rinse out separator from last sampling. Once the separator had been rinsed out for a couple of minutes the vapor vent was adjusted so that a blue cone formed at the outlet. The blue cone is an indicator that dry steam is being vented [44]. The water vent was kept at a full opening throughout the sampling process, allowing water level in the separator to remain low to ensure the best quality of the vapor sample. After adjusting the vapor outlet, a silicone hose was attached and rinsed for a couple of minutes before it was attached to the Giggenbach bottle. The silicone hose was fitted with a y-connection and a check valve. The end without the check valve was connected to the bottle

Figure 3.1: Webre seperator at wellhead for vapor phase sampling.

and excess vapor was vented out the other end. The check valve ensured that no air could flow into the flask if sudden loss of flow was experienced in the hose. Every well head was equipped with a small plastic barrel, seen in figure 3.2, filled with cold water for cooling the bottle during sampling. The sampling configuration and Giggenbach glass bottle can be seen in figure 3.2. During sampling the container is kept upside down, so that the vapor travels through the NaOH mixture, and shaken a few times to ensure adequate mixing in the bottle. Each sample collection took about 35-45 minutes and the bottle was filled with condensate and NaOH mixture up to the curvature at the top if possible. Some wells did not have the power to fill the flask to the desired end point, for those wells the sampling was terminated when bubbles stopped rising through the liquid.

3.1.2 Liquid phase sampling methods

Compared to the vapor phase sampling process the liquid phase sampling process was a simple one. Instead of using a Webre separator a simple separator was used, seen in figure 3.3. The separator consisted of a pipe and a narrow outlet where the liquid was dispensed. The vapor phase escaped at the top due to its light density while the liquid dropped to the bottom where the sample was taken. Again, each wellhead was equipped with its own separator. An empty bucket was placed below the sampling line outlet to catch all extra liquid. The separator was attached to the wellhead upside down and the sampling line valve carefully opened for flow. By placing the separator upside down, any dirt in the sampling line was let out through the large opening of the separator to avoid it clogging the liquid outlet. Once the liquid flowing from the well had turned clear, the sampling line valve was closed, and separator flipped to the correct orientation. The opening of the valve had to be carefully adjusted so that only steam was escaping at the top and liquid flowing out the bottom. Once the valve opening had been adjusted the separator was rinsed out for a couple of minutes to avoid contamination from the previous sampling.

Figure 3.2: Sampling set up, bottle upside down and water for cooling.

Figure 3.3: Separator for liquid phase sampling.

Liquid samples were collected in airtight amber glass bottles. The liquid phase samples were untreated, thus no preparation was needed before heading out to the field. Once the separator had been cleaned out the sample flask was rinsed out three times with the geothermal fluid before the sample was taken. The sample bottle was filled completely and the cap tightened. The samples were then stored until they were sent to ÍSOR to be analyzed.

3.2 Analytical methods

All samples were analyzed by ÍSOR using their equipment and techniques. The following two sections will describe in detail what methods were used to analyze the samples and calculate SF6, 2,7-NDS and 2,6-NDS concentrations.

3.2.1 Vapor phase sample analytical methods

The SF6 samples were analyzed using a Thermo Scientific Trace 1310 gas chromatograph equipped with a TG Bond Alumnia Na_2SO_4 analytical column and an electron capture detector (ECD). 99.999% pure nitrogen was used as both make-up and carrier gas. The preferred software for instrumental control and data analysis was Chromeleon, version 7.2. The injection and oven temperatures were kept at 373 kelvin and 333 kelvin respectively. Injection time for each sample was 1 minute and run-time was kept at 7 minutes.

The method used to calculate the concentration of SF_6 in the samples is based on the same principle as many chemical analytical methods. The detector in the gas chromatograph yields a spectra with a peak for the analyte. Thus, the first step was to run the samples from the field through the gas chromatograph and achieve a spectra for each sample. The second step was to create a standard curve by running a series of samples with a known concentration of SF_6 through the gas chromatograph. The standard curve correlates the area of the peak to number of moles of SF_6 in the samples from the field. Using the ideal gas law the number of moles in the injection line can be calculated:

$$n_{line} = \frac{P_{line}V_{line}}{RT} \tag{3.1}$$

Where n_{line} is the total number of moles in the injection line, P_{line} is the pressure of the sample in the injection line in millibar, V_{line} is the volume of the injection line in milliliters, R is the gas constant in milliliter-millibar/kelvin-mol and T is the temperature of the sample in kelvin. Here the volume of the injection line was 28.68 mL.

When the standard curve is created the standard gas is injected at different pressures to vary the number of moles in the injection line. Since the concentration of SF_6 in the standard is known, in this case 1 ppm, the total number of moles SF_6 in the known volume of the sampling line can be calculated:

$$n_{line\mathrm{SF_6}} = 1x10^{-6}n_{line} \tag{3.2}$$

Once enough data points have been obtained to create a standard curve with peak areas of the same scale as those of the unknown samples, analysis of the unknown samples can begin. The standard curve used in this particular case is presented in figure 3.4.

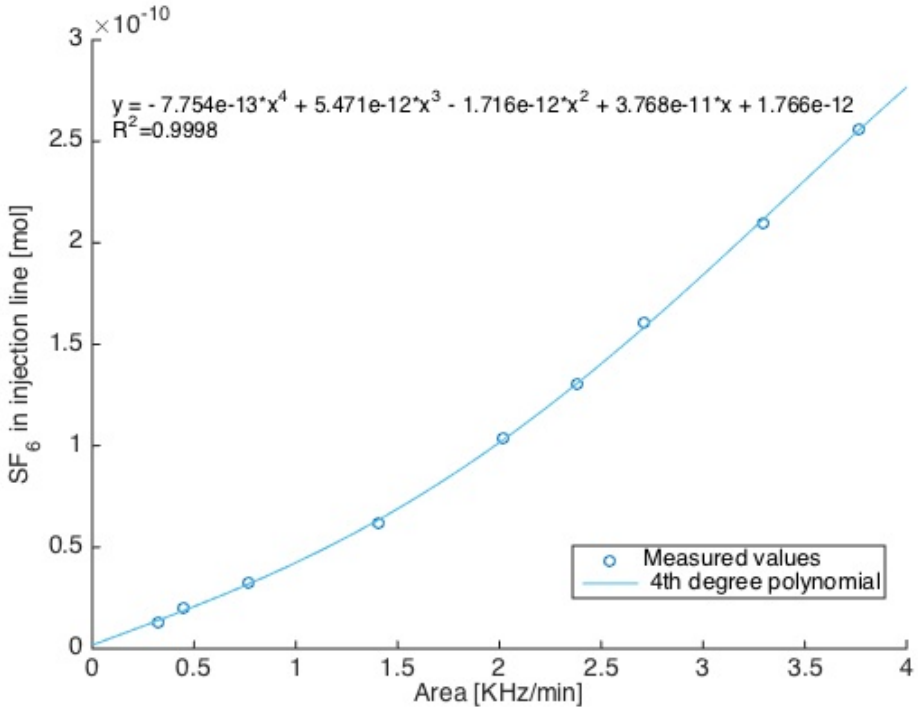

Figure 3.4: Standard curve that correlates peak areas to number of moles in injection line, data provided by ÍSOR.

Using the standard curve, the number of moles in the sampling line for the unknown concentration can now be calculated. Once $n_{line\mathrm{SF_6}}$ is known, the volume of the headspace in the sample is calculated. Before each flask was used, it was weighed before the addition of NaOH and after evacuation as described in section 3.1.1. After sampling, the flask was weighed again and the weight recorded. This information was used to calculate the volume of the headspace in the flask using equation 3.3:

$$V_{hs} = V_f - \frac{(m_{full} - m_{empty})}{\rho_{NaOH}} \tag{3.3}$$

Where V_{hs} is the volume of the headspace in milliliters, V_f is the volume of the sampling flask, ρ_{NaOH} is the density of the NaOH solution in g/mL, m_{full} is the mass of the flask after sampling in grams, m_{empty} is the mass of the empty flask in grams.
During each run the temperature and pressure of the injection line and the sample flask are equal. Thus, Avogadros's law can be applied to calculate the number of moles in the sample:

$$n_{\mathrm{SF_6}} = n_{line\mathrm{SF_6}} \frac{V_{total}}{V_{line}} \tag{3.4}$$

Where V_{total} is given by:

$$V_{total} = V_{hs} + V_{line} \tag{3.5}$$

Once the number of SF_6 moles in the sample have been calculated, the mass of SF_6 in the sample is calculated using the molar mass of SF_6:

$$m_{SF_6} = M(\mathrm{SF_6}) n_{\mathrm{SF_6}} \tag{3.6}$$

Where m_{SF_6} is the mass of SF_6 in grams, and $M(SF_6)$ is the molar mass of SF_6, which is equal to 146.06 g/mol. Finally, the mass fraction of SF_6 in the sample is calculated. Here

the first step is to calculate the total sample mass:

$$m_{sample} = (m_{full} - m_{evacuated})\frac{kg}{1000g} \tag{3.7}$$

where m_{sample} is the mass of the sample in kg, m_{full} is the mass of the flask after sampling in grams and $m_{evacuated}$ is the mass of the flask after evacuation. Once the mass of the sample itself is known the mass fraction in the sample can be calculated:

$$c = \frac{m_{SF_6}}{m_{sample}} \tag{3.8}$$

where c is the mass fraction in $g/kg_{condensate}$.

The limiting factor for the method was high concentration of standard gas available compared to the peak areas of the unknown samples. The samples with a concentration below approximately 0.02 ppb (or $2x10^{-5}$ mg/kg condensate) could not be analyzed with a high degree of certainty. The reason for this is that those concentrations fall below the scope of the available standard curve, and due to non-linearity of the data, extrapolation can not be guaranteed.

3.2.2 Liquid phase analytical methods

The liquid phase samples were analyzed in a high performance liquid chromatograph (HPLC) using fluorescence spectroscopy at the ÍSOR lab. The HPLC solution used was a UlitMate 3000 from Dionex, equipped with a 50 mm x 2.1 mm BetaBasic column from Dionex and a fluorescent detector [45]. The detector's excitation wavelength was set at 225 nm and emission wavelength was set at 340 nm. Injector volume for the HPLC was 20 µg and flow rate between 0.5-0.7 mL/min. The system pressure was 170-190 bar. The mobile phase consisted of phosphate buffer in methanol/water mixture. The phosphate buffer consisted of 3.17 mM Na_2HPO_4, 6.21 mM KH_2PO_4 and 5.0 mM $(CH_3CH_2CH_2CH_2)_4N[OP(OH)_2O]$ (TBAP). The methanol/water mixture consisted of 25% methanol and 75% water. This HPLC method resulted in chromatographic separation of 2,6 NDS and 2,7 NDS from each other and from reservoir interferences [46]. The runtime for each sample was 15 min.

To clean the samples before each run they were filtered using a 0.22 µm nylon filter. Before each run 5 standards mixed with geothermal brine from SV-7 were run through the UltiMate 3000. Those standards were 0.1 ppb, 0.5 ppb, 1 ppb, 5 ppb and 10 ppb. Additionally, the 5 standards were run through the system after every 10th sample. The detection limit of 2,6 NDS and 2,7 NDS in the HPLC was 0.2 ppb.

3.3 Modeling methods

The main goal with this paper is to increase the understanding of the characteristics of the Svartsengi geothermal system and estimate the risk of a cold front due to the current reinjection into the field. In order to do that the tracer returns were modeled quantitatively using a couple of programs included in the ICEBOX software package. The programs that were used were TRINV, for simulating tracer returns, and TRCOOL, for creating long term cooling predictions in production wells.

3.3.1 Tracer transport

The TRINV software was developed by Orkustofnun and has been used successfully in numerous geothermal fields around the world [47], [48], [10]. The software is based on principles of the theory of solute transport, which was discussed in detail in section 2.1, and on the basis of one dimensional flow-channel model [10]. In reality wells are connected by complex nets of fracture-zones, interbeds and layers, the one dimensional flow channel model, however, assumes that the flow between an injection well and a production well can be modeled by one or more flow channels. These one dimensional flow channels are used to describe the parts of these structures that are relevant to each pair of injection and production wells. Since the model assumes flow only in one direction, the differential equation for tracer transport equation 2.5 can be simplified to [10]:

$$D\frac{\partial^2 C}{\partial x^2} = u\frac{\partial C}{\partial x} + \frac{\partial C}{\partial t} \tag{3.9}$$

Where D is the dispersion coefficient in m^2/s given by equation 3.10, C is the tracer concentration in the channel in kg/m^3 at a distance x, x is the distance along the flow channel in meters, and u is the average fluid velocity given in m/s, described by equation 3.11. In the model mechanical dispersion is assumed to dominate molecular dispersion, thus the dispersion coefficient is given by:

$$D = \alpha_L u \tag{3.10}$$

Where α_L is the longitudinal dispersivity of the channel in meters and u is average fluid velocity given by:

$$u = \frac{q}{\rho A \phi} \tag{3.11}$$

Where q is the injection flow rate in the flow channel in kg/s, ρ is the geothermal fluid density in kg/m^3, A is the average cross-sectional area of the flow channel in m^2 and ϕ is the porosity of the channel.

If some amount of tracer , M, is assumed to be injected instantaneously and molecular diffusion is ignored, tracer concentration in the production well is given by [10],[47], [49]:

$$c(t) = \frac{uM_r\rho}{Q}\frac{1}{2\sqrt{\pi Dt}}e^{(-(x-ut)^2/4Dt)} \tag{3.12}$$

Where M_r is the tracer mass flowing along the channel in kg, Q is the production rate in kg/s and x is the distance between the injection well and production well in meters.

The conservation of mass law correlates the tracer concentration in the production well to the tracer concentration in the fracture zone, and is the basis for simulating the tracer return data with equation 3.12 [50],[10]:

$$c(t)Q = C(t)q \tag{3.13}$$

Where $c(t)$ is the concentration of tracer in the production well fluid in kg/m^3, Q is the production rate in kg/s, $C(t)$ is the concentration of tracer in the flow channel and q is the injection flow rate in the flow channel in kg/s.

In cases where the production well and injection well are connected by more than one flow channel equation 3.12 becomes [47], [49]:

$$c(t) = \sum_{i=1}^{n} \frac{u_i M_{r,i} \rho}{Q} \frac{1}{2\sqrt{\pi D_i t}} e^{(-(x_i - u_i t)^2 / 4 D_i t)} \tag{3.14}$$

where $c(t)$ is the concentration of tracer in the produced fluid, n is the number of flow channels $M_{r,i}$ is the tracer mass in flow channel i and x_i the distance along flow-path i. u_i, q_i and D_i are the average linear velocity along flow-path i, flow rate in channel i and the dispersion coefficient in flow-channel i, respectively, given by:

$$u_i = \frac{q_i}{\rho A_i \phi_i} \tag{3.15}$$

$$D_i = \alpha_{Li} u_i \tag{3.16}$$

$$q_i = \frac{M_{r,i}}{M} q_{inj} \tag{3.17}$$

where A_i is the cross-sectional area of flow-path i, ϕ_i is the porosity of channel i, α_{Li} is the longitudinal dispersivity of flow-channel i and q_i is the flow of geothermal fluid in flow-path i, and q_{inj} is the injection rate.

The name of the software,TRINV, stands for tracer inversion. The flow channel properties are the flow channel cross-sectional area ($A_i \phi_i$), the flow channel dispersivity (α_{Li}) and the flow channel length (x). During the modeling the flow channel length is fixed as the distance between the main feed-zones of the two wells involved. As the name indicates, the software solves equations 3.14-3.17 inversely using a non-linear least squares fitting to simulate the tracer return data and obtain the model parameters [10], [47]. The one-dimensional flow channel model does not yield a unique solution to the problem, especially when considering multiple flow channels. Thus, a thorough understanding of the system and the tracer test data is required when analyzing the solutions and estimating the most likely solution to the problem [47].

Once the most probable solution has been determined, TRCOOL is used to make cooling predictions. The TRINV program gave information about the flow channels in the system. This information is part of the input into the TRCOOL program. Temperature changes due to long term reinjection are dependent on the properties of the flow channels, not only their volume but mainly on porosity and surface area [10]. Thus, in order to get the most accurate predictions of the temperature decline, those parameters need to be estimated by looking at geological and geophysical data from the field.

3.3.2 Thermal breakthrough

The reservoir rock matrix acts as a heat exchanger when water colder than reservoir conditions is injected into the system. The capacity of the heat exchanger depends on the contact surface area between the rock and the fluid, the heat capacity of both the rock and the geothermal fluid, and the thermal conductivity of the rock. Thermal breakthrough can be predicted using a similar equation to the one describing advancement of tracers. The thermal changes can be described using equation 3.18 [51]:

$$R_{thermal} \frac{\partial T}{\partial t} + u \cdot \nabla T = \kappa \nabla^2 T \tag{3.18}$$

where κ is the thermal diffusivity in m^2/s and $R_{thermal}$ is the unitless thermal retardation coefficient. κ and $R_{thermal}$ are further defined by

$$R_{thermal} = 1 + \frac{(1-\phi)\rho_R c_R}{\phi \rho_w c_w} \tag{3.19}$$

and

$$\kappa = \frac{k_{th}}{\phi \rho_R c_R} \tag{3.20}$$

where ρ_R is the density of the rock in kg/m^3, c_R is the specific heat capacity of the rock in J/Kg/°C, ϕ is the unit-less porosity of the rock matrix and k_{th} is the thermal conductivity of the formation in W/m/°C.

Studies on the propagation of a thermal front in single phase, porous medium have shown that due to the thermal inertia of the rock volume, the thermal front lags behind the fluid front by a constant factor related to the volumetric heat capacity [51],[52],[53]. In other words, in homogeneous media, free of diffusive and dispersive effects, a sharp transition from the reservoir temperature to injection temperature should be expected behind the injection front. The mixing of geothermal and injection fluid, however, is largely controlled by diffusive or dispersive effects that cause both an earlier and more gradual decrease in the production temperature.

If we imagine a simple conceptual model shown in figure 3.5 describing transport along a fissure then the thermal transport can be described by [54]:

$$R_{thermal}\frac{\partial T_f}{\partial t} + u\frac{\partial T_f}{\partial x} - D\frac{\partial^2 T_f}{\partial x^2} - \frac{\kappa'_m}{b}\frac{\partial T_m}{\partial y}\bigg|_{y=b} = 0, |y| \leq b \tag{3.21}$$

and

$$\frac{\partial T_m}{\partial t} = \kappa_m \frac{\partial^2 T_m}{\partial x^2}, |y| > b \tag{3.22}$$

.

where T_f is the temperature withing the fracture zone matrix and T_m is the temperature in the rock matrix. Here κ_m is the thermal diffusivity in the rock matrix outside the fracture, further defined as

$$\kappa_m = \frac{k_{th}}{\phi \rho_m c_m} \tag{3.23}$$

where ρ_m is the density of the rock matrix outside the fracture and c_m is the specific heat capacity of the rock matrix outside the fracture.

κ'_m is the thermal diffusivity within the fracture zone matrix, similarly defined as

$$\kappa'_m = \frac{k_{th}}{\phi \rho_f c_f} \tag{3.24}$$

where the subscript f denotes properties of the fracture zone material. Note that the fracture is not completely free of rock and open to flow of pure geothermal fluid.

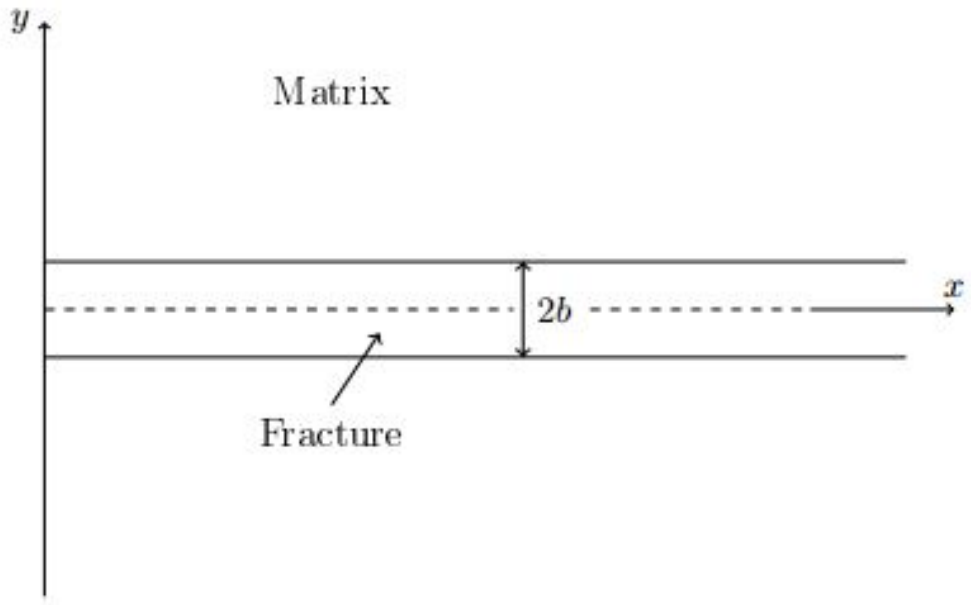

Figure 3.5: Diagram of an idealized single fracture matrix system [54].

In the model presented here, the mechanical dispersion term from the tracer model above has been retained. However, in a solution presented by Carslaw and Jaeger [55] the dispersion is assumed to have an insignificant effect on thermal breakthrough. For steady flow conditions the production temperature, $T_P(L,t)$ becomes:

$$T_P(L,t) = T_0 - \omega_{inj}\frac{q}{Q}(T_0 - T_I)\,\mathrm{erfc}\left[\frac{k_{th}L/(\phi\rho_w c_w)}{2bu\sqrt{\kappa_m(t - R_{thermal}x/u)}}h\left(\frac{ut}{R_{thermal}} - x\right)\right] \quad (3.25)$$

Where T_0 is the initial formation temperature in °C, ω_{inj} is the fraction of injected fluid reaching the production well, which is equal to the ratio M_i/M, T_I is the temperature of injected fluid in °C, L is the length of the flow channel in meters, b is half the width of the fracture-zone in meters, and h is the height of the flow-path inside the fracture-zone in meters. Note that for multiple flow channels the solution is:

$$T_P(L,t) = T_0 - \sum_{i=1}^{n}\omega_{inj,i}\frac{q_i}{Q}(T_0 - T_I)\,\mathrm{erfc}\left[\frac{k_{th}L_i/(\phi_i\rho_w c_w)}{2b_i u_i\sqrt{\kappa_{m,i}(t - R_{thermal,i}x_i/u_i)}}h_i\left(\frac{u_i t}{R_{thermal,i}} - x_i\right)\right] \quad (3.26)$$

The equations presented above (eq. 3.25 and 3.26) are valid at times $t > \frac{R_{thermal}x}{u}$.

The solution presented here above is the one used by TRCOOL to predict thermal breakthrough in production wells based on tracer test data. Several parameters control the arrival of thermal changes, including the thermal retardation factor, the fracture opening, the porosity of the channel and the matrix diffusivity. However, the fraction of injected fluid reaching the well, the production rate and the temperate difference between the reservoir and injected fluid sets the limit for the magnitude of cooling. In this solution dispersion is assumed to have an insignificant affect on the thermal breakthrough. However, it should be noted that in reality dispersion does in fact play a role in the process. By including the dispersive part in the solution it is possible that an improved prediction would be achieved.

The results of the tracer test is used to estimate the average linear velocity in the fracture (u) and the cross-sectional area ($A\phi$). From there assumptions are often made about the surface area available for heat transfer. It is recommended that this be done for at least two extremes. One where the surface area is small, or a pipe like flow channel, this would result in the most rapid cooling prediction. The other scenario would be a larger surface area flow channel, similar to a thin horizontal layer, that is a more optimistic scenario resulting in slower cooling. Reasonable estimates of the formation density, heat capacity, and thermal conductivity can either be found by using likely values from the literature or measuring samples from the formation. In this case the likely values from the literature will be used due to the long research and production history of Svartsengi. An estimate of the fracture porosity can often be found in the literature, but if no such value is available a conservative value should be used in order to avoid underestimating the onset of thermal breakthrough [54]. The fracture porosity, along with the fracture aperture and unforeseen changes in the flow field due to production are the most uncertain parameters affecting the thermal breakthrough predictions.

When thermal breakthrough predictions are made based on tracer tests the underlying assumption is that the fluid and temperature fronts follow the same paths from injection to extraction wells. One must keep in mind that over the course of long term production of a geothermal field this assumption may not be valid [54]. Chemical changes in the reservoir fluid, pressure drawdown and thermal changes due to production can alter flow-paths in the reservoir. Decreased reservoir temperatures within the field can lead to increased viscosity of the reservoir fluid and consequently slow down the thermal breakthrough [56]. However, significant changes to viscosity are more pronounced in cases where the temperature changes are very drastic. Thus, this phenomenon is unlikely to have a considerable effect on the thermal breakthrough predictions. Another factor that might alter flow paths in the reservoir are varying flow rates, such as injection and production rates. During geothermal utilization the injection and production rates are bound to vary to some extend and that was indeed the case over the duration of this tracer test, as will be illustrated further in section 4.1. The model however is not designed to account for large variations on production or injection rates, thus average rates were used for the analysis of the data.

Chapter 4

Results

4.1 Tracer recovery

In this section the tracer recovery in different wells will pe presented. The amount of recovered tracer will also be calculated and the concentration of tracer in production wells will be discussed.

Before the data can be analyzed in any way the tracer recovery must be estimated for each production well of the test. The amount of tracer throughout the test was estimated based on equation 4.1:

$$m_i(t) = \int_0^t c_i(s)Q_i(s)ds \tag{4.1}$$

where $m_i(t)$ is the cumulative mass recovered in production well i in kg at time t, c_i is the tracer concentration in the production well in kg/L or kg/kg and Q_i is the production rate of the well i in L/s or kg/s.

At the time of writing liquid tracer has only been detected in small concentrations in two samples, both from SV-9, thus minimum discussion will be on the results of the liquid tracer test as it is still ongoing. 2,6-NDS was detected in both samples, but no 2,7-NDS was detected. Preliminary observations indicate that the injected fluid from SV-24 does arrive in the production wells slightly quicker than fluid injected into well SV-17.

The first step in determining the tracer return was to gather information about the production from each well over the duration of the test. Due to annual maintenance stops that overlapped with the test, variation in production rates were rather large, as seen in figure 4.1. Wells SV-10, SV-16, SV-20 and SV-23 produce purely from the steam zone while SV-22, SV-11 and SV-7 are wet steam wells. In order to calculate the portion of steam in the wet steam wells a couple of different methods were used. According to HS ORKA (personal communication with Ómar Sigurðsson), the enthalpy of well SV-22 is around 1850 kJ/kg. Using the enthalpy of the well and steam tables the quality of the steam was determined using the following equation:

$$x_v = \frac{h_{geof} - h_f}{h_g - h_f} \tag{4.2}$$

where x_v is the vapor quality, h_{geof} is the enthalpy of geothermal fluid in the well (1850 kJ/kg), h_f is the enthalpy of saturated liquid state and h_g is the enthalpy of saturated vapor

state. At the separator pressure of 5.5 bar the value of h_f and h_g are 655.4 kJ/kg and 2752.8 kJ/kg, respectively [57]. According to equation 4.2 the vapor fraction in well SV-22 is 0.57, which is in agreement with a value obtained by Þorvaldsson et al. [3]. For wells SV-7 and SV-11 values published by [3] were used, considering how recent the data was and how well calculations for SV-22 matched up to it. It was determined that these numbers were an accurate description of the current status of those two wells. Both wells produce about 22.4% steam and 81.6% fluid at the separator pressure. Using these fractions new production numbers for steam only were calculated and presented in figure 4.2.

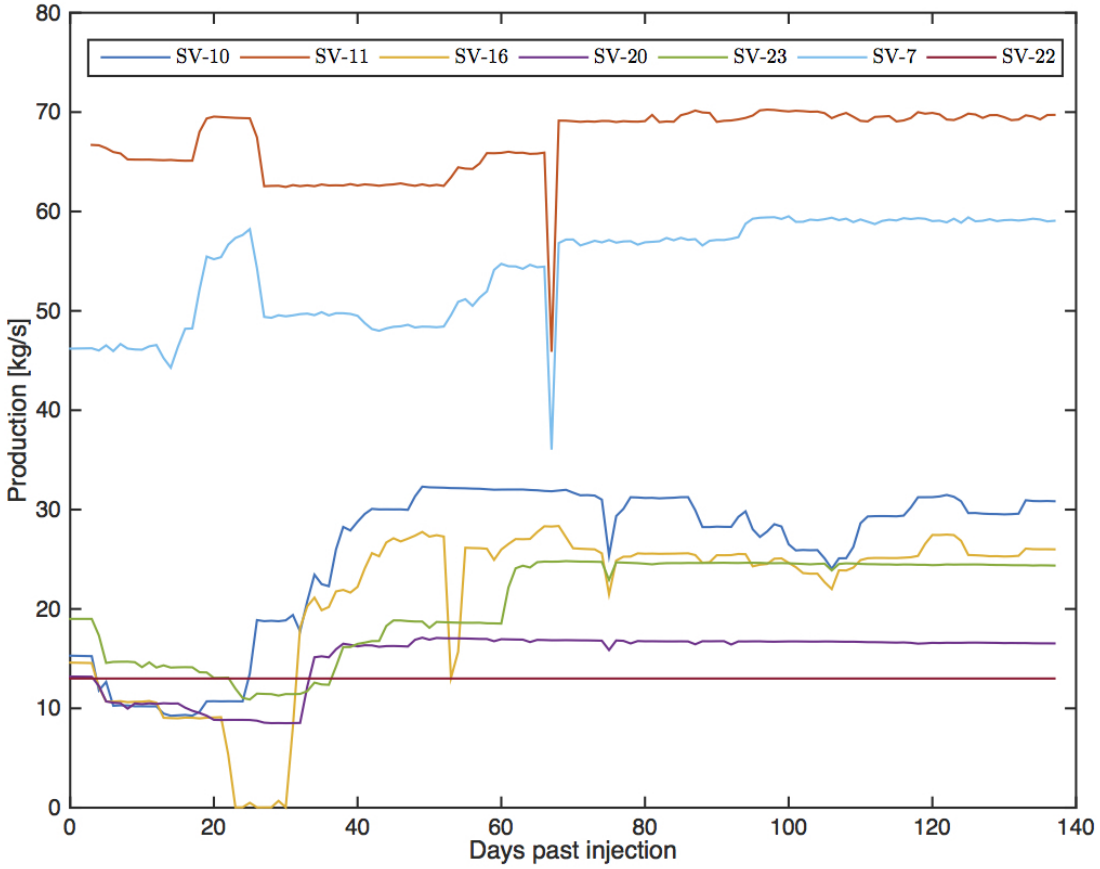

Figure 4.1: Production variations throughout the steam phase test

One of the objectives of this thesis was to determine whether the appropriate amount of tracer was injected. For best results the concentration of tracer in the production wells should reach at least 5-10 times the detection limit, at the peak concentration in the well. The lowest area for the 1 ppm standard is 0.32 kHz/min, which yields a concentration around $2x10^{-8}$ $g/kg_{condensate}$, or 0.02 ppb [8]. Despite the detection limit of the equipment being lower than 0.02 ppb, samples with concentrations below 0.02 ppb could not be analyzed with a high degree of accuracy. Thus 0.02 ppb is taken as the reference point here. Approximately 60% of the samples, where SF_6 was detected, yielded a spectra with a peak area below 0.32 kHz/min. In order to create a standard curve for samples with such a low concentration using a 1 ppm standard the gas had to be put under a pressure down to 10 mbar, in other words, down to the lowest pressure the equipment capable of. This created a higher risk of error incorporated into the standard curve. According to test that were performed at ÍSOR to evaluate the standard curve the deviation was in the range of -5.3% - 7.2%.

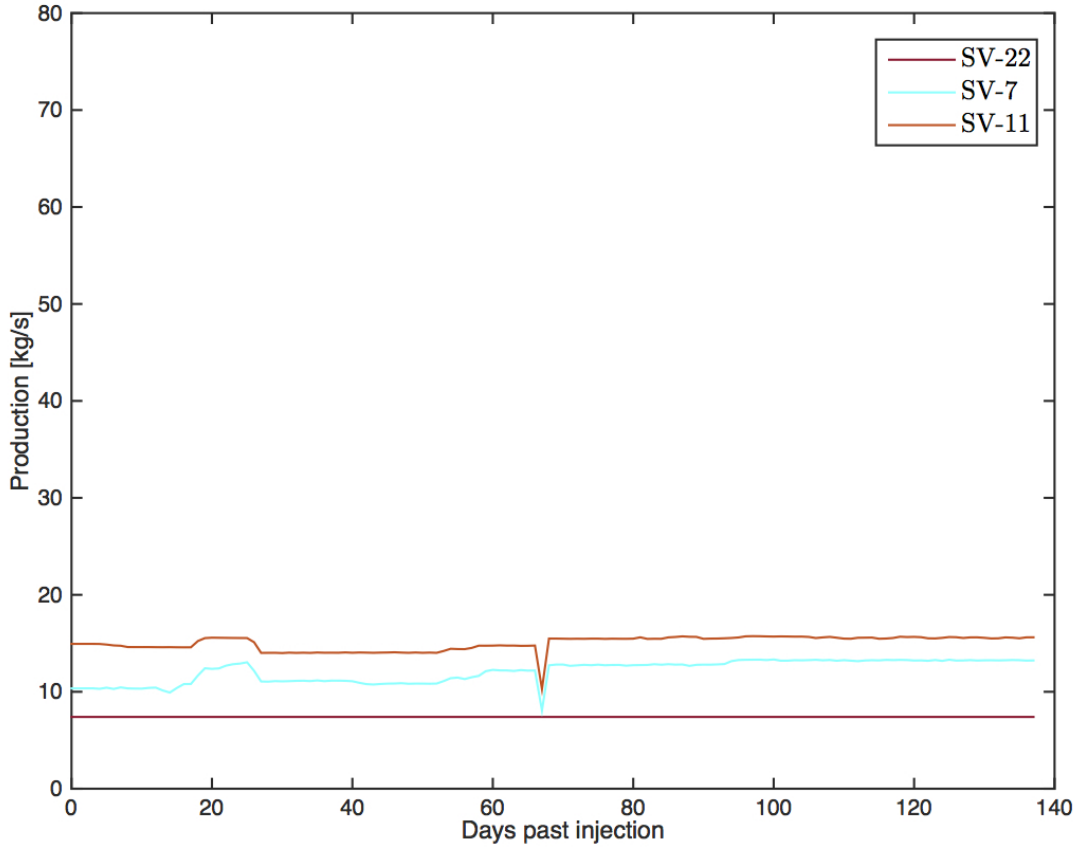

Figure 4.2: Steam phase production for wet steam wells

Using techniques explained in section 3.2.1, the concentration of SF_6 was calculated in $g/kg_{condensate}$, as presented in figure 4.3. The highest peak in SV-11 corresponds to $3x10^{-7}$ $g/kg_{condensate}$ and the peak in SV-23 corresponds to $2x10^{-7}$ $g/kg_{condensate}$. Those two peaks do indeed reach a concentration of 5-10 fold the detection limit. However, the only other well to reach a concentration 5 times the limit, is well SV-16. Due to the fact that a large number of samples have a concentration right at or just under the detection limit and the low concentration forced the standard gas to be worked with at low pressures that introduced additional error into the standard curve, it is evident a larger amount of SF_6 should have been used in the steam phase tracer test at Svartsengi.

The amount of tracer recovered throughout the test was calculated based on eqn.4.1 and data presented in figures 4.1, 4.2 and 4.3. First signs of SF_6 showed up on day 17 in wells SV-7 and SV-11. Four days later the tracer was detected in all other wells in the Svartsengi production field, except for SV-20 where no sampling was scheduled until the next day and the first signs of SF_6 were detected. Over the duration of the steam phase sampling no tracer was detected in the Eldvörp exploration well.

A minimal amount of tracer was recovered in the production wells, or only about 0.035% of the injected tracer. The largest amount of tracer, 7.7 g, was recovered in well SV-23 as seen in figure 4.4. SV-11 came next with 6.5 g recovered while the smallest amount of tracer (0.5 g) was recovered in SV-22. The total recovery was estimated to be 28.9 g out of 86.78 kg of injected tracer. Even though, samples were taken from well SV-14 for the first 5 weeks of the test, the well was not in operation and thus no returns were calculated.

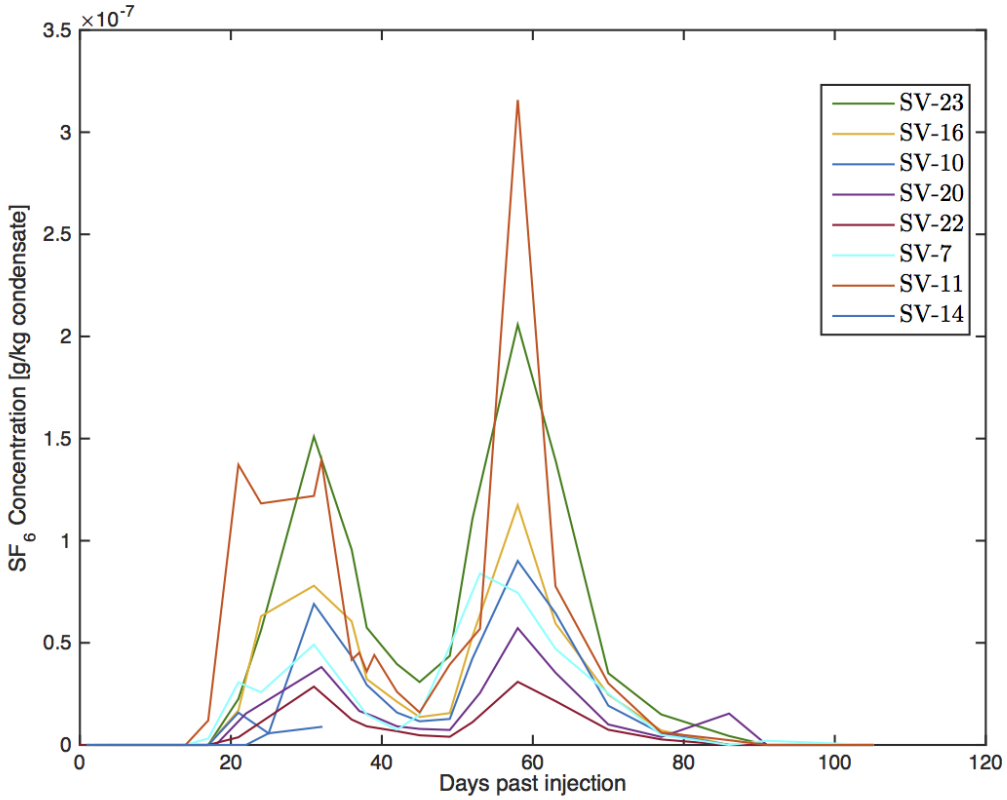

Figure 4.3: Concentration of SF_6 in production wells

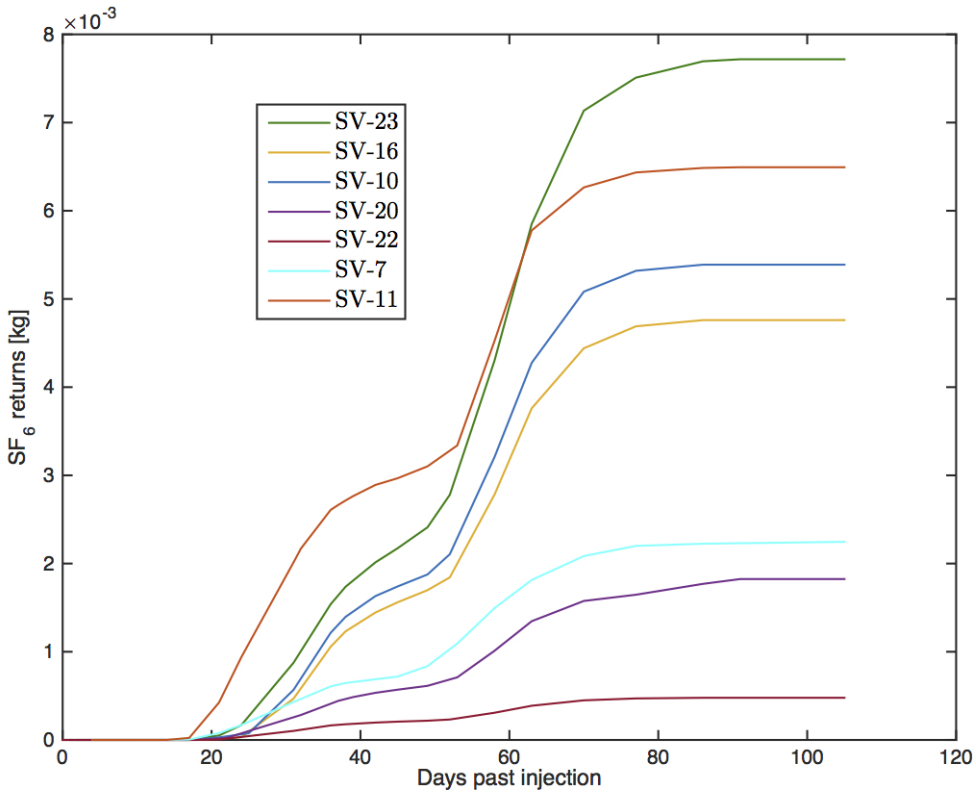

Figure 4.4: Cumulative SF_6 returns per well

The low recovery of tracer is most likely a consequence of several different factors. First off, the steam zone at Svartsengi is quite large and the tracer has the ability to spread over large area. Thus entering fractures or channels that do not reach the production wells. Another reason can be that a portion of the tracer travels with the liquid phase and does not enter the steam phase in production wells. Finally, once it was evident that recovery of the tracer was extremely low more research was done on the success rate of using SF_6 as a tracer in geothermal fields. In tests reporting distances above approximately 400 meters, the recovery of the tracer became very low [58], [49]. Another study done at the Geysers in California, where the results of tracer tests using the hydrofluorocarbons R- 134a, R-23 and R-13 and SF_6 were compared, showed that the hydrofluorocarbons had a considerably better recovery than the SF_6 [59]. Thus, despite its theoretical stability in environments below 300°C, SF_6 most likely does experience considerable losses when longer distances are involved.

4.2 Modeling

4.2.1 Steam phase tracer returns

As stated in a an earlier section the arrival of SF_6 was first noted in wells SV-7 and SV-11 17 days after injection and 4 days later in all wells but EG-2. Two separate peaks were noted in all wells in the Svartsengi field, except well SV-14 where sampling was terminated prematurely. In general the first peak was lower but broader than the second peak. The 1st peak arrived in all wells on day 31 or 32, depending on which day the sampling landed, and the second peak arrived in all wells but SV-7 on day 58. The second peak arrived first in well SV-7 on day 53, 5 days before all other wells, but the drop off was not a as quick as in other wells. Therefore, an accurate travel path for SF_6 was impossible to determine. However, as was to be expected, the arrival of the tracer was first noted in the two wells closest to the injection site (SV-7, SV-11), but interestingly higher concentrations of the tracer were experienced in the steam zone wells SV-10, SV-16 and SV-23 than in SV-7 where the tracer was first noted.

In the following subsections the tracer recovery modeling will be discussed in further detail and flow channel parameters will be presented. It should be noted that tracer recovery calculated in the flow channel model, does not match the tracer recovery calculated in the previous section. The one dimensional flow channel model is not equipped to handle large fluctuation in production rates thus an average production rate was used for wells in the modeling section instead of actual rates. In later sections where tracer recovery is mentioned, the recovery using actual flow rates are used.

4.2.1.1 Analysis of two phase wells

The tracer was first noted in wells SV-7 and SV-11 and the highest concentration of tracer was measured in well SV-11. This is not surprising when looking at the distances between wells, as these two wells are located over 500 m closer to SV-24 than the next steam phase or two phase well as seen in table 2.1. The high concentration indicates the largest degree of connection between SV-11 and SV-24 out of all the wells. Figure 4.5 shows the observed and simulated SF_6 recovery in well SV-11 and the model parameters are shown in table 4.1. The second largest tracer recovery was obtained in well SV-11, due to an average production rate of 15 kg/s. With two flow channels the models show an average match, with a coefficient of determination of 92.6%, mainly due to scatter in the first peak. Due to very small surface area the flow velocity is very high, or 91 m/day for the first channel and 44 m/day for the second

channel. Attempts were made to simulate the tracer recovery using three flow channels but proved unsuccessful. Despite higher concentrations experienced in the second channel slightly more tracer is recovered in the lower and broad peak in the first channel.

Table 4.1: Parameters of the flow channel model simulating the tracer recovery in well SV-11.

Channel Number	**1**	**2**
Average flow velocity, u [m/s]	$1.06x10^{-3}$	$5.08x10^{-4}$
Average flow velocity, u [m/day]	91	44
Longitudinal dispersivity,α_L [m]	68.7	3.1
Tracer mass, M_i [kg]	$3.26x10^{-3}$	$1.96x10^{-3}$
Length, x [m]	2450	2550
Cross section, $A\phi$ [m^2]	$2.40x10^{-1}$	$3.01x10^{-1}$
Mass fraction, M_i/M [%]	$3.75x^{-3}$	$2.26x10^{-3}$

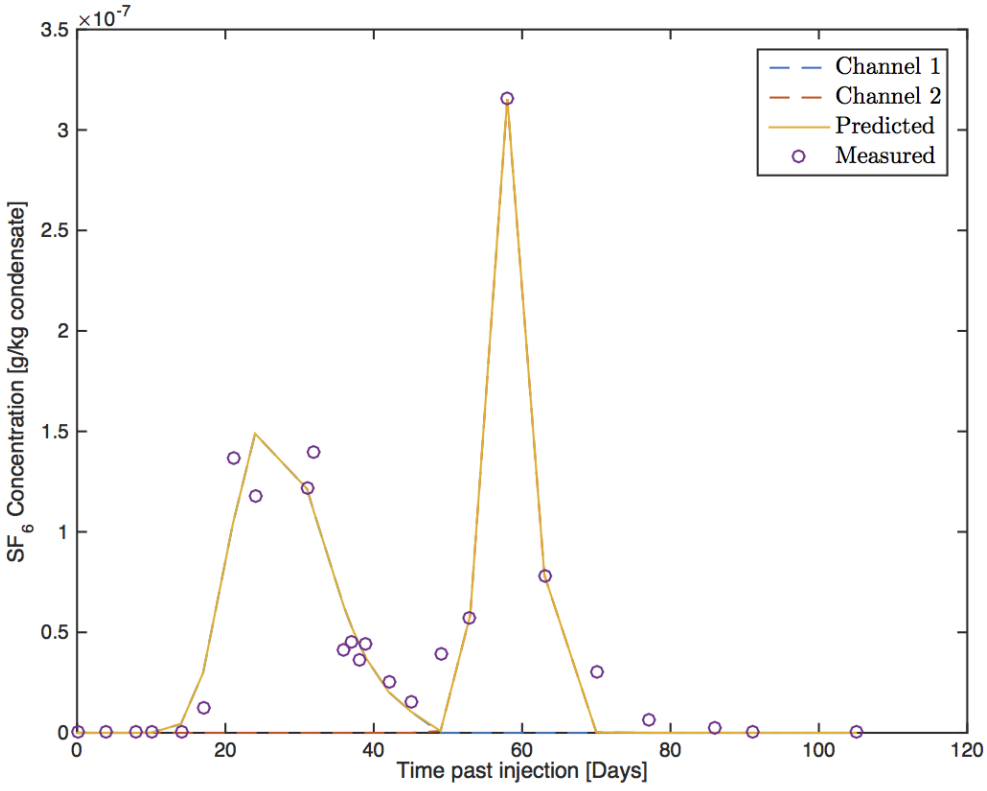

Figure 4.5: Observed and simulated SF_6 recovery in well SV-11

The tracer concentration in SV-7 was considerably lower than in SV-11 despite being located only 200 m NE of SV-11. Tracer recovery in the well was also relatively low, partly due to a low production rate of 12 kg/s. Flow velocities were comparable to velocities in well SV-11, or 92 m/day and 48 m/day, as seen in table 4.2 along with other model parameters. Again two channels with small cross-sections were used to model the recovery with a fairly good match with a coefficient of determination of 95.5%, see figure 4.6.

Table 4.2: Parameters of the flow channel model simulating tracer recovery in well SV-7.

Channel Number	**1**	**2**
Average flow velocity, u [m/s]	$1.06x10^{-3}$	$5.56x10^{-4}$
Average flow velocity, [m/day]	92	48
Longitudinal dispersivity,α_L [m]	57.5	19.8
Tracer mass, M_i [kg]	$7.54x10^{-4}$	$1.48x10^{-3}$
Length, x [m]	2618	2700
Cross section, $A\phi$ [m^2]	$5.54x10^{-2}$	$2.08x10^{-1}$
Mass fraction, M_i/M [%]	$8.69x10^{-4}$	$1.71x10^{-3}$

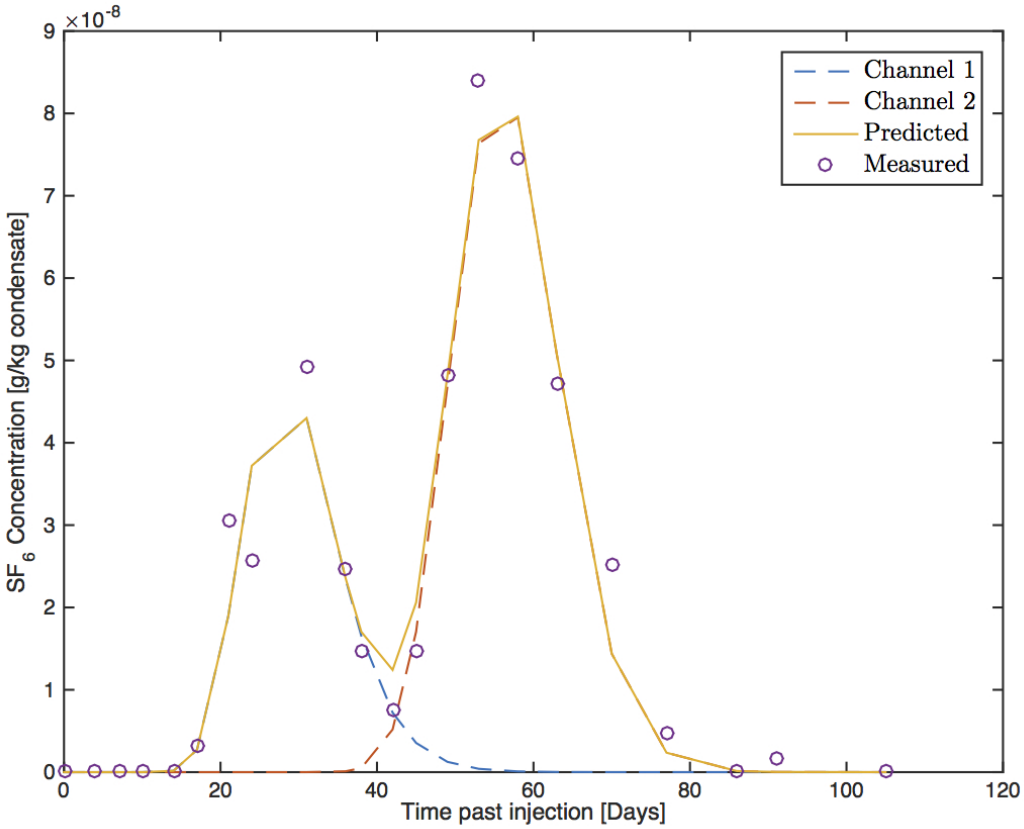

Figure 4.6: Observed and simulated SF_6 recovery in well SV-7

The two phase well with the lowest tracer concentration was SV-22, which was also the well with the lowest average production rate over the duration of the test with 7.4 kg/s. The well is directionally drilled, away from the injection well. At the bottom of the well it is 3333 m away from SV-24 and is furthest away of all the production wells. The cross sectional areas of the flow channels used to model the recovery (see table 4.3), were smaller than the cross sectional area in wells SV-7 and SV-11, but comparable. The coefficient of determination using two flow channels was 95.1%. Again the model showed a fairly good match as seen in figure 4.7. Of all the wells the connectivity between the injection well and the production well is the lowest in well SV-22.

Table 4.3: Parameters of the flow channel model simulating tracer recovery in well SV-22.

Channel Number	**1**	**2**
Average flow velocity, u [m/s]	$1.13x10^{-3}$	$6.65x10^{-4}$
Average flow velocity, [m/day]	98	57
Longitudinal dispersivity,α_L [m]	38.7	12.8
Tracer mass, M_i [kg]	$2.12x10^{-4}$	$2.51x10^{-4}$
Length, x [m]	3023	3333
Cross section, $A\phi$ [m^2]	$1.46x10^{-2}$	$2.94x^{1}0^{-2}$
Mass fraction, M_i/M [%]	$2.44x10^{-4}$	$2.89x10^{-4}$

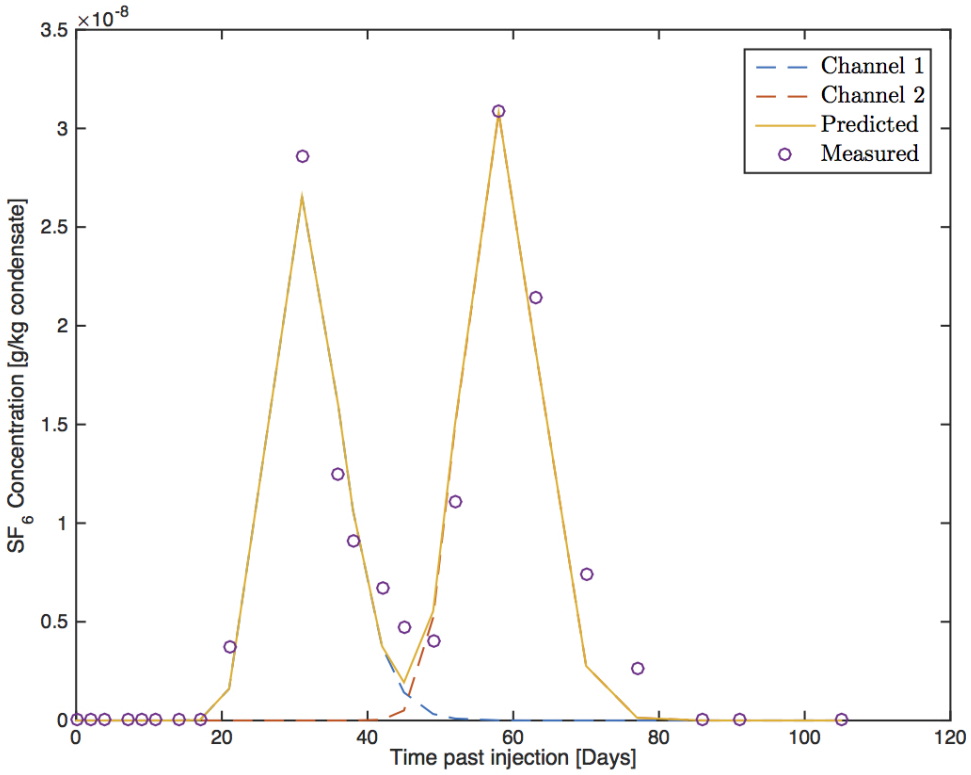

Figure 4.7: Observed and simulated SF_6 recovery in well SV-22

Both wells SV-7 and SV-11 had rather broad first peaks, with a bit of scatter in the data. This might indicate that two different channels are feeding the wells during the first peak that caused the rise and drop in concentration. However, despite efforts to model the data using more than two flow channels no such results were achieved. That can partly be the result of the limited number of data points and the small concentrations of tracer involved. Well SV-22 is located considerably closer to steam zone wells than the other two phase wells at Svartsengi. The recovery in SV-22 looked more similar to the recovery curves in the steam zone wells, that will be presented in the next subsection, than the recovery curves in its fellow two phase wells.

4.2.1.2 Analysis of steam zone wells

Despite the long distance between SV-23 and SV-24, and being directionally drilled away from the injection well, SV-23 was the well with the second highest concentration and the

largest recovery of tracer. The relatively large recovery of tracer can be traced back to a high average production rate of 19 kg/s and the high concentration of tracer in the well. Interestingly, the cross sections of both the first and second channel were the largest of all wells. Table 4.4 shows the model parameters used for both channels. A very good match was obtained for the model, coefficient of determination of 99.1%, as seen in figure 4.8.

Table 4.4: Parameter of the flow channel model simulating tracer recovery in well SV-23

Channel Number	**1**	**2**
Average flow velocity, u [m/s]	$1.16x10^{-3}$	$6.56x10^{-4}$
Average flow velocity, [m/day]	100	57
Longitudinal dispersivity,α_L [m]	49.9	15.2
Tracer mass, M_i [kg]	$3.37x10^{-3}$	$4.69x10^{-3}$
Length, x [m]	3096	3288
Cross section, $A\phi$ [m^2]	2.27x10−1	$5.57x10^{-1}$
Mass fraction, M_i/M [%]	$3.88x10^{-3}$	$5.41x10^{-3}$

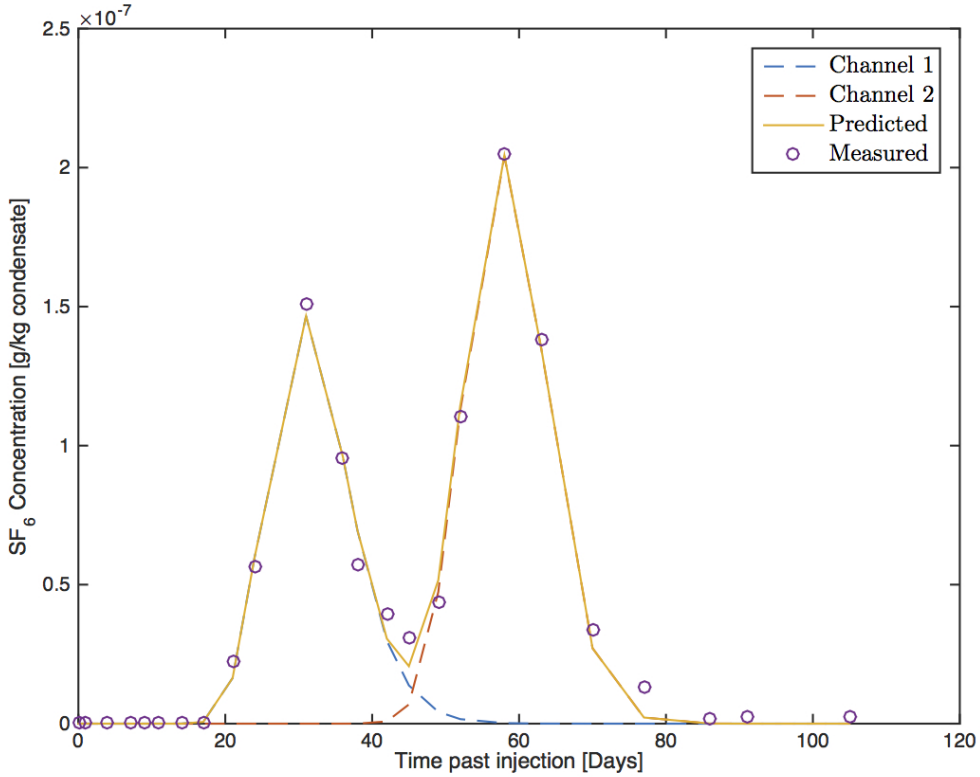

Figure 4.8: Observed and simulated SF_6 recovery in well SV-23.

SV-10 is located 3244 m away from the injection well. Over the duration of the test average flow rate in the well was 28 kg/s. Judging from the tracer concentration in each well, the connectivity between SV-10 and SV-24 is average compared to other wells in the field. Due to high production rates the third largest amount of tracer was recovered in well SV-10. The model parameters are presented in table 4.5. The model proved a fairly good match to the measured data, or with a coefficient of determination of 97.1%, as seen in figure 4.9.

Table 4.5: Parameter of the flow channel model simulating tracer recovery in well SV-10

Channel Number	**1**	**2**
Average flow velocity, u [m/s]	$1.22x10^{-3}$	$6.53x10^{-4}$
Average flow velocity, [m/day]	105	56
Longitudinal dispersivity,α_L [m]	34.3	14.4
Tracer mass, M_i [kg]	$1.87x10^{-3}$	$2.98x10^{-3}$
Length, x [m]	3255	3274
Cross section, $A\phi$ [m^2]	$1.20x10^{-1}$	$3.56x10^{-1}$
Mass fraction, M_i/M [%]	$2.16x10^{-3}$	$3.44x10^{-3}$

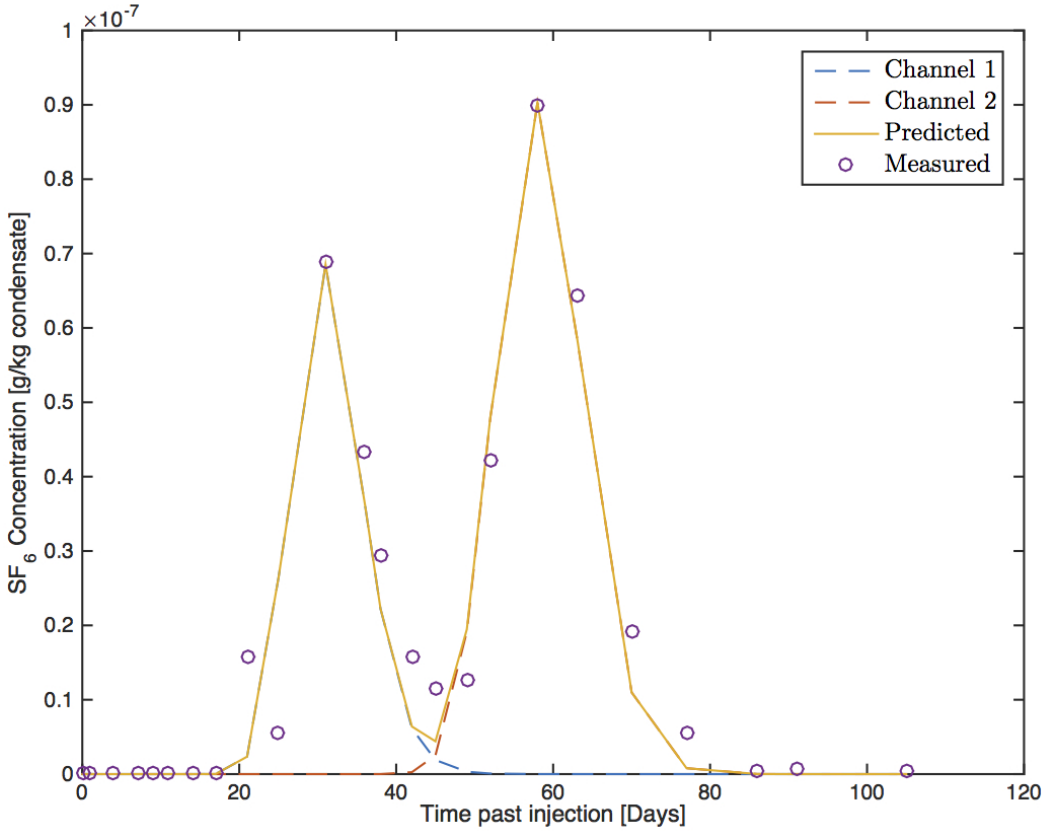

Figure 4.9: Observed and simulated SF_6 recovery in well SV-10.

The average production rate over the duration of the test was 20 kg/s in well SV-16. The connectivity between SV-16 and SV-24 is the third greatest of all wells in terms of concentration of tracer in well. The coefficient of determination for the simulation was 97.3%, as seen in 4.10. Model parameters are presented in table 4.6.

Table 4.6: Parameter of the flow channel model simulating tracer recovery in well SV-16.

Channel Number	**1**	**2**
Average flow velocity, u [m/s]	$1.28x10^{-3}$	$6.65x10^{-4}$
Average flow velocity, [m/day]	111	57
Longitudinal dispersivity,α_L [m]	70.7	10.7
Tracer mass, M_i [kg]	$2.33x10^{-3}$	$2.29x10^{-3}$
Length, x [m]	3294	3316
Cross section, $A\phi$ [m^2]	$1.42x10^{-1}$	$2.69x10^{-1}$
Mass fraction, M_i/M [%]	$2.68x10^{-3}$	$2.64x10^{-3}$

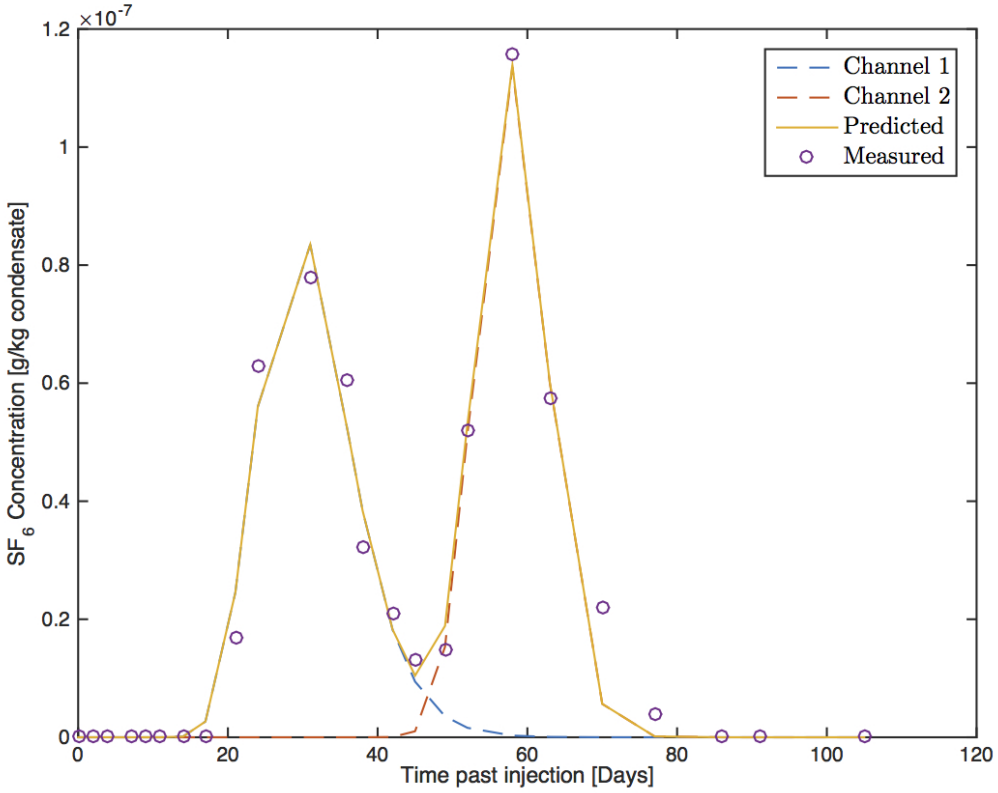

Figure 4.10: Observed and simulated SF_6 recovery in well SV-16.

The average flow rate in well SV-20 over the duration of the test was 16 kg/s. In terms of tracer concentration and flow channel cross-sectional area (see table 4.7), well SV-20 has the second lowest degree of connectivity to the injection well. A surprisingly high tracer concentration was measured towards the end of the test, as seen in figure 4.11. Attempts were made to fit the data using three channels but proved unsuccessful, thus it cannot be determined whether this last data point is noise in the data or an actual increase in the well's tracer concentration. The coefficient of determination using two flow channels was 93.5%.

Table 4.7: Parameter of the flow channel model simulating tracer recovery in well SV-20.

Channel Number	**1**	**2**
Average flow velocity, u [m/s]	$6.37x10^{-4}$	$1.27x10^{-3}$
Average flow velocity, [m/day]	55	109
Longitudinal dispersivity,α_L [m]	11.3	64.2
Tracer mass, M_i [kg]	$9.43x10^{-4}$	$8.46x10^{-4}$
Length, x [m]	3235	3250
Cross section, $A\phi$ [m^2]	$1.15x10^{-1}$	$5.20x10^{-2}$
Mass fraction, M_i/M [%]	$1.09x10^{-3}$	$9.74x10^{-4}$

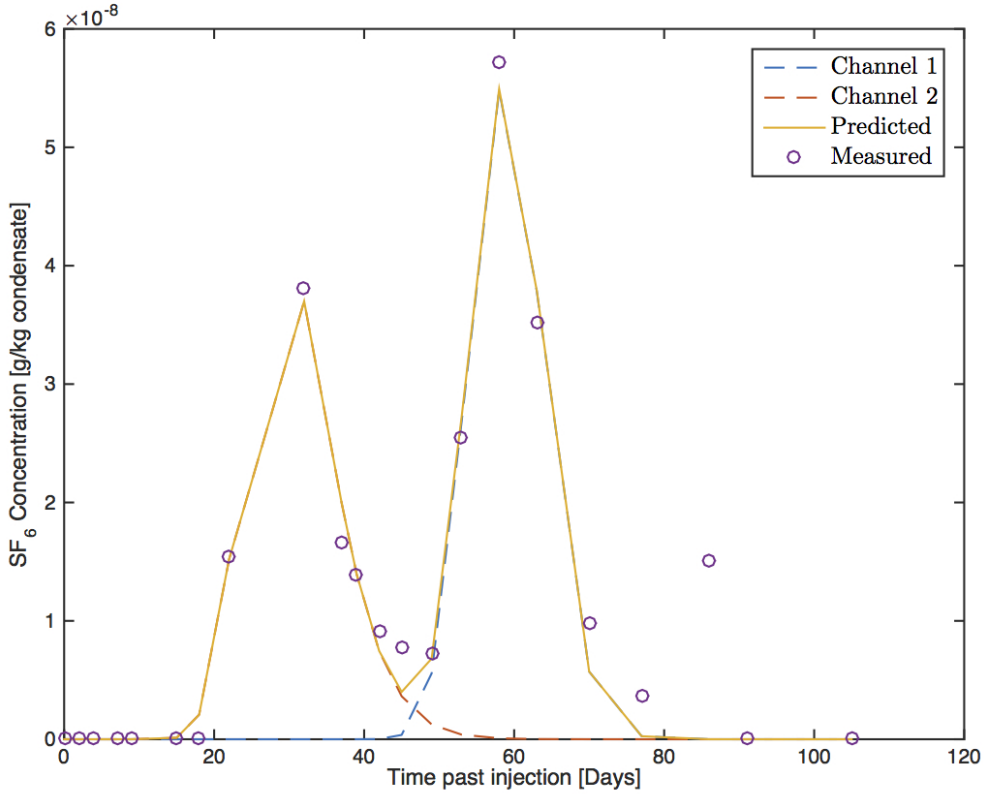

Figure 4.11: Observed and simulated SF_6 recovery in well SV-20

In general, less scatter in the data was noted in the first peak of the tracer recovery for steam zone wells than two phase wells and over all better model fits were achieved. More similarity was noted between the two peaks than between the two peaks in the two phase wells and in all cases but one, two flow channels seemed to be an appropriate description of the recovery. Here, well SV-20 was the out-lier with a relatively large concentration of tracer in the third to last sample when the concentration in previous samples was lower.

4.2.2 Liquid phase tracer returns

At the time of writing 2,6-NDS had only been detected in two samples, and no traces of 2,7-NDS have been detected in the production wells. Both samples containing 2,6-NDS above detection limits were from well SV-9.

Due to the limited number of samples available for modeling, no attempts were made to model the liquid phase tracer recovery as the tracer tests are still ongoing.

4.3 Cooling predictions

Shortly into the modeling process, it became apparent, due to the very modest recharge from the injection well to production wells, that thermal breakthrough in steam zone and two phase wells due to reinjection into SV-24 was highly unlikely. However, in order to get a better idea of how the injection would affect the field temperature if reinjection was continued at its current rate for the next 30 years, cooling predictions were made using TRCOOL from the ICEBOX software package. Additionally, predictions were made for the extreme case of doubling the reinjection into well SV-24.

As stated in section 3.3.2, the fracture porosity and the fracture aperture, or the geometry, are two of the most uncertain parameters affecting the thermal breakthrough predictions. Since tracer tests do not give any information about the flow channel geometry, it is often recommended that cooling predictions should be made for 2-3 different scenarios to deal with that uncertainty. The three scenarios often used are represented in table 4.8. For this study only the pessimistic scenario was used due to the small cross-sectional area of predicted flow channels.

Table 4.8: Recommended assumptions for cooling predictions.

Scenario	Outlook	Surface Area	Porosity
1	Optimistic	Large	Low
2	Intermediate	Large	High
3	Pessimistic	Small	High

Porosity in the Svartsengi field is believed to range from 5% to 40%, but generally a porosity of 15% is considered to be high [60]. Thus an average porosity of 15% was used for these calculations. Presented in table 4.9 are the model parameters assumed in this study.

Reinjection of 95°C condensate brine mixture into well SV-24 was started in 2008, and since then no effects of cooling have been experienced. As expected, thermal breakthrough predictions showed that insignificant cooling would be expected due to reinjection at a current rate. For example the two wells that would experience the greatest amount of cooling were wells SV-23 and SV-11 with a cooling of 0.1°C. When the injection rate was doubled the model predicted a cooling of 0.2°C. This insignificant cooling is because the tracer test indicates that only a tiny fraction of the injected fluid reaches the production wells. However, one should keep in mind that if the tracer return was underestimated, due to SF_6 escaping the system or being lost during injection for example, cooling predictions would be underestimated and not detect a possible cold front within the 30 year lifetime.

Table 4.9: Flow channel model parameters used to predict cooling.

Well	Channel Length [m]	Height [m]	Width [m]	Porosity [%]
SV-7	2618	2.4	0.6	15
	2700	1.3	0.3	15
SV-11	2450	2.8	0.7	15
	2550	2.9	0.7	15
SV-10	3255	2.0	0.5	15
	3274	3.0	0.8	15
SV-16	3294	2.0	0.5	15
	3316	2.6	0.7	15
SV-20	3235	0.9	0.2	15
	3250	1.3	0.3	15
SV-22	3023	0.6	0.2	15
	3333	0.9	0.2	15
SV-23	3096	2.5	0.6	15
	3288	3.9	1.0	15

Chapter 5

Conclusions

The three simultaneous tracer tests at Svartsengi, described and analyzed in this thesis, were carried out with the purpose of gaining a better understanding of the connections between the two injection wells, SV-17 and SV-24, and the production wells at Svartsengi and research well at Eldvörp. In total fourteen production and research wells were sampled during the test. Thereof, five steam phase wells, four two phase wells and five liquid phase wells. At the time of writing, six months after the injection of liquid and steam tracers at Svartsengi, steam phase sampling has been terminated and the steam phase tracer is believed to have completed its journey to the monitored wells. The steam phase tracer was detected in all production wells at Svartsengi at very low concentration but no signs of SF_6 were noted in the research well in Eldvörp. Well SV-14 was shut in a short time into the test and, therefore no analysis was done on the results from SV-14.

First signs of 2,6-NDS showed up on December 16th, 177 days past injection, in well SV-9 with a measured concentration of 0.5 ppb. Since then one other sample from the same well with a concentration of 0.9 ppb has been analyzed. No signs of 2,7-NDS have been detected. Due to the limited amount of data available, no modeling or analysis of the liquid phase tracer recovery was attempted.

In total 0.035% of the injected steam tracer has been recovered. This very low recovery indicates an extremely modest recharge from SV-24 to the wells producing from the steam phase of the reservoir. A possible contributor to the low recovery of the tracer is that a part of the SF_6 is lost despite its theoretical stability at the reservoir temperature, as was discussed in section 4.1. A portion of the tracer could also travel with the liquid phase and not enter the wells producing from the steam zone. A large number of data points were measured right around the detection limit of the equipment and technology available. Recommendations made in section 2.1 state that concentration of the tracer in production wells should reach at least 5-10 times the detection limit. According to that recommendation the tracer test meets that demand in wells SV-11 and SV-23 during the highest peaks. However, due to the low concentration in other wells and number of measurements that fall right around the detection limit of the tracer, a larger amount of steam phase tracer should have been injected into the system in order to obtain more reliable results. The low concentrations involved caused a rather high standard deviation curve for the SF_6, in the range of -5.3%-7.2%. Another way to mitigate this large error would have been to use a standard gas of lower concentration than 1 ppm, which was not available at the time. Higher pressures would have been needed to create the appropriate standard curves using a gas of lower concentration, thus reducing the

risk of error incorporated into the standard curve.

The greatest concentration was experienced in well SV-11, the well located closest to the injection well. The largest recovery on the other hand was in well SV-23, located relatively far from the injection well. For all wells a two flow channel model was used to model the recovery with adequate coefficient of determination. Attempts were made to model the tracer recovery using a larger number of flow channels, but they were unsuccessful. That was in part due to the low percentage and concentration of tracer recovered. The width and variability in the recovery curves indicates that most likely a larger number of flow channels are feeding the production wells from SV-24. Well SV-7 and SV-11 both have two separate peaks in the early half of the test, arriving at similar times indicating the possibility of at least two different pathways. A large number of steam zone wells have very wide first and second peaks, giving rise to the possibility of multiple pathways.

Due to the fast flow velocity of the tracers, between 91-111 m/day for the first channel and between 44-57 m/day for the second flow channel, and relatively low sampling frequency, exact mapping of the sequence of arrival and travel paths between production wells could not be determined. Based on the large difference between arrival time of steam tracer and liquid tracers, it is believed that the steam phase and liquid phase do not travel together for a significant distance. In section 2.2.2 the steam zone at Svarsengi was described and a possible conceptual model of the steam zone at earlier stages of development shown (see figure 2.5). It is known that the steam zone has spread further out into the field since the start of production at Svartsengi due to a pressure drawdown in the field, causing SV-7 and SV-11 to produce two phase flow. The large time difference between the arrival of the steam tracer and the liquid tracer indicates that the steam phase travels at a higher rate through the system and enters steam layer rather soon after injection, where it travels to wells SV-11 and SV-7, before spreading to other wells in the field. The steam zone was believed to have formed originally due to fractures linked to a N-S fault in the caprock of the reservoir. Thus, allowing up flow of geothermal fluid into the upper part of the reservoir, the fluid was then spread to production wells via NE-SW faults. The relatively high concentration of tracer in SV-23 compared to surrounding wells indicates the directionally drilled well cuts the steam zone close to its origin, where the steam flows up to the steam zone wells. From there the greatest flow is into well SV-16 and SV-10. Other wells in the zone (SV-14, SV-20, and SV-22 producing both from steam and liquid zones) are further away from the origin, receiving less concentrations of tracer and producing less steam over the duration of the test. In this regard little connection was seen between the distance of production well from injection well, but rather connection to their location in the steam zone.

The absence of steam tracer in Eldvörp does not rule out a connection and pressure support that has been noted in the two fields in so many studies before, as was discussed in section 2.2.1 and 2.3. All the extraction in the area is happening to the ENE of the injection wells while the research well at Eldvörp is located to the WSW of the injection wells. Thus, it can be expected that the flow gradient is higher towards the production wells at Svartsengi than towards Eldvörp, minimizing tracer transport into the research well at Eldvörp.

The two channel flow models indicated an extremely small cross-sectional area of the pathways, with the largest combined cross-sectional area for the two flow channels being $0.78\,m^2$ in well SV-23. The longitudinal dispersion in all simulations indicates a medium to low dispersion in the flow channels. However, due to the low recovery it is likely that

the injected fluid that enters the steam phase diffuses and disperses through the reservoir outside direct flow channels. The steam zone has extended quite far out at Svartsengi and the reservoir rock is highly permeable compared to many other geothermal reservoirs. Thus, the steam has the ability to disperse over a large area and a large part of the steam does not reach the production wells in the timeframe of this study, contributing the low recovery of the tracer.

One of the main purposes of this study was to determine the risk of thermal breakthrough due to present reinjection. Thirty year cooling predictions were made using the two channel model parameters. The 95°C brine condensate mixture is injected into the 240°C reservoir at a rate of about 115 kg/s through well SV-24. Recommendations were made in section 4.3, where three different scenarios were presented. Because of the small portion of injected fluid reaching the production wells only the most pessimistic outlook was used. The initial goal was to create thermal breakthrough predictions for current injection rate, lower injection rate, and a higher injection rate. However, once predictions had been made for the current scenario and double the current injection rate it became clear that predictions for lower injection rates were unnecessary. The thirty year cooling predictions for 115 kg/s indicated that a cooling of less than a tenth of a degree should be expected in all wells, with the largest degree of cooling in SV-23 and SV-11. When the injection rate was doubled the expected cooling increased to less than two tenths of a degree. The result from this test state that the injection can be continued at this current rate, or even double the current rate, without significant cooling in the production wells within the next 30 years. However, it is possible the recovery of the tracer was underestimated. In that case cooling predictions are also underestimated and the risk of thermal breakthrough might not have been detected. Thus, liquid tracer returns need to be analyzed in conjunction with steam tracer returns for a more accurate prediction.

5.1 Recommendations

An objective of this paper was to gather information about the success of the tracer test and make recommendation about which elements can be improved upon, which will be the subject of this section.

Air contamination was noted in majority of the samples throughout the whole test. Numerous attempts were made in order to find the source of the contamination but all were unsuccessful. For future tracer tests using the same methods, and possibly the same equipment, a thorough study with the goal to eliminate such a contamination should be performed prior to the start of the test.

Additional risk of error was introduced into the standard curve due relatively low concentrations of SF_6 in the samples. The low tracer concentration and high concentration of standard gas available, forced the use of lower than desirable pressures in the creation of standard curves. The low pressures created standard curve errors between -5.3%-7.2%. To mitigate this error a larger amount of tracer needs to be injected in conjunction with the use of a standard gas of a lower concentration than 1 ppm.

The steam phase tracer traveled rather quickly through the system and few data points were obtained during the rise and drop of peak values. The sampling of the steam phase tracer is quite time consuming and it can be tempting to minimize the sampling frequency as quickly as possible for various reasons. In this case a higher sampling frequency, where

samples would have been taken at least once daily, would have provided valuable data and a better continuity for the modeling of the tracer recovery.

Another improvement related to the modeling and calculations of the tracer recovery would have been to perform the test at a time that does not coincide with annual maintenance stops. Maintenance stops cause large fluctuation in production rates which the flow channel model is not equipped to handle. For the analysis of a tracer test with such fast recoveries, stable production rates are preferred.

Finally, research in the field should be continued and the data already obtained from the steam phase tracer should be evaluated with the liquid phase tracer once sampling has been terminated. The liquid phase data can provide important information about the direction of flow in the field, connections between liquid and steam phase transports, and has the ability to give a different view on the risk of thermal breakthrough.

Bibliography

[1] S. Þórhallsson, T. Hauksson, S. P. Kjaran, M. Ólafsson, and A. Albertsson, "Niðurdæling í Svartsengi frá tilraunum til stöðugs rekstrar", presented at the Málþing Jarðhitafélags Íslands, 2004.

[2] J. S. Guðmundsson, T. Hauksson, S. Thorhallsson, A. Albersson, and G. Thorolfsson, "Injection and tracer testing in Svartsengi field, Iceland", in *Well Session*, New Zealand: New Zealand Geothermal Workshop, 1984, pp. 175–180.

[3] L. Þorvaldsson, E. M. Myer, and A. Arnaldsson, "Svartsengi- Reykjanes: Vinnslueftirlit fyrir árið 2014", Vatnaskil Consulting Engineers, Iceland, Tech. Rep. 15.06, 2015, p. 44.

[4] HS Orka, "Ársskýrsla 2008- financial statement 2008", HS Orka, Iceland, Annual Report, 2008, p. 152.

[5] ——, "Ársskýrsla 2014", HS Orka, Iceland, Annual Report, 2015. [Online]. Available: `http://arsskyrsla2014.hsorka.is/` (visited on 12/02/2015).

[6] S. Þórhallsson and S. P. Kjaran, "Niðurdæling í háhitasvæðið Svartsengi", in *Jarðhiti-Rannsóknir*, Reykjavík, Iceland, Nov. 1991, pp. 361–382.

[7] S. S. Gylfadóttir, "Svartsengi - Reykjanes : Hita- og þrýstingsmælingar 2013", Íslenskar orkurannsóknir, Reykjavík, Tech. Rep. ÍSOR-2014/026, 2014, p. 84.

[8] E. Eyjólfsdóttir, *Analyses of SF6 and calculations*, Memorandum, May 11, 2015.

[9] L. Þorvaldsson and A. Arnaldsson, *Svartsengi-30 year production scenarios*, Memorandum.

[10] G. Axelsson, G. Björnsson, and F. Montalvo, "Quantitative interpretation of tracer test data", presented at the Proceedings World Geothermal Congress 2005, Antalya, Turkey, 2005.

[11] S. S. Einarsson, A. Vides, and G. Cuéllar, "Disposal of geothermal waste water by reinjection", presented at the Second United Nations Symposium on the Development and Use of Geothermal Resources, San Francisco, California, USA, 1975, pp. 1349–1355.

[12] G. S. Bodvarsson and V. Stefansson, "Some theoretical and field aspects of reinjection in geothermal reservoirs", *Water Resources Research*, vol. 25, no. 6, pp. 1235–1248, Jun. 1, 1989.

[13] V. Stefánsson, "Geothermal reinjection experience", *Geothermics*, vol. 26, no. 1, pp. 99–139, Feb. 1997.

[14] G. M. Shook, S. L, and A. Wylie, "Tracers and tracer testing: Design, implementation, tracer selection, and interpretation methods", Idaho National Laboratory (INL), Tech. Rep. INEEL/EXT-03-01466, Jan. 1, 2004.

[15] J. Bear, *Hydraulics of Groundwater*. Courier Corporation, Mar. 15, 2012, 594 pp.

[16] J. Bear, D. I. Zaslavskii, and S. Irmay, *Physical Principles of Water Percolation and Seepage*. Unesco, 1968, 480 pp.

[17] D. K. Todd and L. W. Mays, *Groundwater Hydrology*. Wiley, 2005, 636 pp.

[18] I. Javandel, C. Doughty, and C.-F. Tsang, *Groundwater transport: Handbook of mathematical models*. American Geophysical Union, 1984, 244 pp.

[19] Vatnaskil, "Conceptual model of development of the Svartsengi-Eldvörp-Reykjanes geothermal reservoirs", Vatnaskil Consulting Engineers, Reykjavík, Tech. Rep. 12.01, Mar. 2012, p. 39.

[20] M. H. Jenness and A. E. Clifton, "Controls on the geometry of a holocene crater row: A field study from southwest Iceland", *Bulletin of Volcanology*, vol. 71, no. 7, pp. 715–728, Feb. 17, 2009.

[21] C. R. Pullinger, "Geological and geothermal mapping at Nupafjall and Svartsengi, Reykjanes peninsula, SW-iceland", UNU Geothermal Training Programme, Final 11, 1991, p. 45.

[22] L. S. Georgsson and H. Tulinius, "Viðnámsmælingar á utanverðum Reykjanesskaga 1981 og 1982", Orkustofnun, Reykjavík, Tech. Rep. OS-83049/JHD-09, Jun. 1983.

[23] R. Karlsdóttir, "TEM-viðnámsmælingar á utanverðum Reykjanesskaga", Orkustofnun, Reykjavík, OS-97001, Apr. 1997, p. 63.

[24] S. P. Kjaran, J. Elíasson, and G. K. Halldórsson, "Svartsengi: Athugun á vinnslu jarðhita", Orkustofnun, Reykjavík, Tech. Rep. OS80021/ROD10-JHD17, Jun. 1980.

[25] J. Elíasson, S. S. Arnaldsson, and S. P. Kjaran, "Svartsengi : Straumfræðileg rannsókn á jarðhitasvæði", Orkustofnun, Reykjavík, Tech. Rep. OS ROD 7718/OS SFS 7702, 1977, p. 74.

[26] H. Franzson, "Svartsengi: Jarðfræðilíkan af háhitakerfi og umhverfi þess", Orkustofnun, Reykjavík, Tech. Rep. OS-90050/JHD-08, Dec. 1990, pp. 1–41.

[27] ——, "Svartsengi jarðfræði holu hsh-14 og tengsl við nærliggjandi holur", Orkustofnun, Tech. Rep. OS-97024, 1997.

[28] B. Richter, S. Þ. Guðlaugsson, B. Steingrímsson, G. Björnsson, J. Ö. Bjarnarson, and S. Þórhallson, "Svartsengi - hola SJ-18 : Borun, rannsóknir og vinnslueiginleikar", Orkustofnun, Reykjavík, Tech. Rep. OS-99117, 1999.

[29] H. Franzson, S. Þ. Guðlaugsson, G. Björnsson, J. Ö. Bjarnason, and S. Þórhallsson, "Svartsengi - hola SJ-17 : Borun, rannsóknir og vinnslueiginleikar", Orkustofnun, Reykjavík, Tech. Rep. OS-99036, 1999.

[30] M. Á. Sigurgeirsson, O. Ó. Kjartansson, H. Björnsson, S. S. Jónsson, and C. Feucht, "Svartsengi - SV-24 : Borun holu SV-24", ÍSOR, Reykjavík, ÍSOR-2008/055, 2008.

[31] G. Björnsson and B. Steingrímsson, "Hiti og þrýstingur í jarðhitakerfinu í Svartsengi : Upphafsástand og breytingar vegna vinnslu", Orkustofnun, Reykjavík, Tech. Rep. OS-91016/JHD-04, 1991.

[32] S. S. Jónsson, S. H. Haraldsdóttir, M. Á. Sigurgeirsson, and B. Richter, "Svartsengi - hola SV-22 : Borun holu SV-22 í 862 m dýpi", ÍSOR, Reykjavík, Tech. Rep. ÍSOR-2008/014, 2008, p. 89.

[33] S. H. Gunnarsdóttir, O. Ó. Kjartansson, S. S. Jónsson, and Christa Feucht, "Svartsengi - hola SV-23 : Borun holu SV-23 í 700 m dýpi", Íslenskar orkurannsóknir, Reykjavík, Tech. Rep. ÍSOR-2008/035, 2008, p. 129.

[34] B. Richter, Á. Guðmundsson, S. Þórhallsson, B. Steingrímsson, G. Ó. Friðleifsson, K. Birgisson, Ó. Sigurðsson, and S. Þ. Guðlaugsson, "Svartsengi, hola SV-20 : Borun vinnsluhluta", Orkustofnun, Reykjavík, Tech. Rep. OS-2002/016, 2002, p. 34.

[35] Schlumberger, *Petrel*, version 2014.4 (64-bit), 2014.

[36] H. Eysteinsson, G. Þorbergsson, and Ó. G. Flóvenz, "Landhæðar- og þyngdarmælingar við Svartsengi og á reykjanesi / hjálmar eysteinsson, gunnar þorbergsson, ólafur g. flóvenz", Orkustofnun, Reykjavík, Tech. Rep. HE-GÞ-ÓGF-91/01, 1991.

[37] H. Eysteinsson, "Elevation and gravity changes at geothermal fields on the Reykjanes peninsula, SW Iceland", presented at the World Geothermal Congress, Kyushu-Tohoku, Japan, 2000.

[38] J. S. Guðmundsson, "Niðurdælingartilraun við Svartsengi 1982", Orkustofnun, Tech. Rep. OS-83047/JDH-07, Jun. 1983, pp. 1–49.

[39] Hitaveita Suðurnesja, "Ársskýrsla 2005-financial statements 2005", Hitaveita Suðurnesja, Iceland, Annual rep. 2006, p. 70. [Online]. Available: `http://www.hsorka.is/HSCompanyInfo/annual_reports/HSOrka_Arsskyrsla2005.pdf` (visited on 07/12/2015).

[40] HS Orka. (2010). HS orka, Energy Plant V, [Online]. Available: `http://hsorka.is/english/HSProduction/Svartsengi/OrkuverV.aspx` (visited on 12/07/2015).

[41] T. Hauksson, "Niðurdælingartilraun í Svartsengi 1984", Orkustofnun, Reykjavík, Tech. Rep. OS-85107/JHD-13, Nov. 1985.

[42] J. S. Guðmundsson and T. Hauksson, "Tracer survey in Svartsengi field 1984", *Geothermal Resource Council: Transactions*, vol. 9.2, pp. 306–315, Aug. 1985.

[43] J. Altamirano, "Sampling and analyses of geothermal steam and geothermometer applications in Krafla, Theistareykir, Reykjanes and Svartsengi, iceland", Tech. Rep. 13, 2006, pp. 153–169.

[44] H. Ármannsson and M. Ólafsson, "Collection of geothermal fluids for chemical analysis", ÍSOR, Reykjavík, ÍSOR-2006/016, 2006.

[45] E. I. Eyjólfsdóttir, *Forvitnast um greiningartæki*, E-mail, Dec. 14, 2015. (visited on 12/15/2015).

[46] P. E. Rose, S. D. Johnson, and P. Kilbourn, "Tracer testing at Dixie valley, Nevada, using 2-napthalene sulfonate and 2,7-napthalene disulfonate", presented at the 26th Workshop on Geothermal Reservoir Engineering, California, USA, 2001, p. 6.

[47] L. Jiurong, "Reinjection and tracer tests in the Laugaland geothermal field, n-iceland", The United Nations University, Geothermal Training Programme, Reykjavík, Tech. Rep. 6, 1999, pp. 141–164.

[48] S. G. Benson, G. M. Aragon, and J. B. Nogara, "Quantification of injection fluids effects to Mindanao geothermal production field productivity through a series of tracer tests, Philippines", presented at the World Geothermal Congress, Indonesia, 2010.

[49] A. I. Molina Martínez and G. Axelsson, "Assessment of thermal interference in the northern part of Los Azufres geothermal field, Mexico, by tracer test analysis", *Geothermal Resource Council Transactions*, vol. 35, pp. 1505–1511, 2011.

[50] G. Axelsson, G. Björnsson, Ó. G. Flovenz, H. Kristmannsdóttir, and G. Sverrisdóttir, "Injection experiments in low-temperature geothermal areas in Iceland", presented at the World Geothermal Congress, 1995.

[51] G. Bodvarsson, "Thermal problems in the siting of reinjection wells", *Geothermics*, vol. 1, no. 2, pp. 63–66, Jun. 1972. (visited on 11/25/2015).

[52] A. W. Woods and S. D. Fitzgerald, "The vaporization of a liquid front moving through a hot porous rock", *Journal of Fluid Mechanics*, vol. 251, pp. 563–579, Jun. 1993.

[53] G. M. Shook, "Prediction of thermal brakthrough from tracer tests", in *24th Workshop on Geothermal Reservoir Engineering*, 1999.

[54] E. K. Bjarkarson, "Predicting thermal drawdown in geothermal systems using inter-well tracer tests", msthesis, Háskóli Íslands, Reykjavik, Feb. 2014, 124 pp. [Online]. Available: `http://hdl.handle.net/1946/17337` (visited on 11/25/2015).

[55] H. Carslaw and J. Jaeger, *Conduction of Heat in Solids*, 2nd. Great Britain: Oxford University Press, 1959, 510 pp.

[56] G. M. Shook, "Predicting thermal breakthrough in heterogeneous media from tracer tests", *Geothermics*, vol. 30, no. 6, pp. 573–589, 2001.

[57] M. J. Moran and H. N. Shapiro, *Fundamentals of Engineering Thermodynamics*, 5th. England: Wiley, 2006, 722 pp.

[58] E. R. Iglesias, M. F. Armenta, R. J. Torres, M. R. Montes, N. R. Picasso, and R. L. Delgado, "Simultaneous liquid- and vapor-phase tracer study in the Tejamaniles area of the Los Azufres, Mexico, geothermal field", presented at the Procedings World Geothermal Congress, Indonesia, 2010.

[59] M. C. Adams, "A comparison of two multiple-tracer tests conducted at the Geysers", presented at the Proceedings 26th Workshop on Geothermal Reservoir Engineering, California, USA, 2011.

[60] J. L. Zuniga, "Geophysical logging in well SG-9, Svartsengi geothermal field, SW-Iceland", UNU Geothermal Training Programme, Reykjavík, Tech. Rep. 1980-8, 1980, p. 79.

School of Science and Engineering
Reykjavík University
Menntavegur 1
101 Reykjavík, Iceland
Tel. +354 599 6200
Fax +354 599 6201
www.ru.is